Molecular Therapy
Nucleic Acids
Original Article

RNA Secondary Structure Motifs of the Influenza A Virus as Targets for siRNA-Mediated RNA Interference

Julita Piasecka,[1] Elzbieta Lenartowicz,[1] Marta Soszynska-Jozwiak,[1] Barbara Szutkowska,[1] Ryszard Kierzek,[1] and Elzbieta Kierzek[1]

[1]Institute of Bioorganic Chemistry, Polish Academy of Sciences, Noskowskiego 12/14, 61-704 Poznan, Poland

The influenza A virus is a human pathogen that poses a serious public health threat due to rapid antigen changes and emergence of new, highly pathogenic strains with the potential to become easily transmitted in the human population. The viral genome is encoded by eight RNA segments, and all stages of the replication cycle are dependent on RNA. In this study, we designed small interfering RNA (siRNA) targeting influenza segment 5 nucleoprotein (NP) mRNA structural motifs that encode important functions. The new criterion for choosing the siRNA target was the prediction of accessible regions based on the secondary structure of segment 5 (+)RNA. This design led to siRNAs that significantly inhibit influenza virus type A replication in Madin-Darby canine kidney (MDCK) cells. Additionally, chemical modifications with the potential to improve siRNA properties were introduced and systematically validated in MDCK cells against the virus. A substantial and maximum inhibitory effect was achieved at concentrations as low as 8 nM. The inhibition of viral replication reached approximately 90% for the best siRNA variants. Additionally, selected siRNAs were compared with antisense oligonucleotides targeting the same regions; this revealed that effectiveness depends on both the target accessibility and oligonucleotide antiviral strategy. Our new approach of target-site preselection based on segment 5 (+)RNA secondary structure led to effective viral inhibition and a better understanding of the impact of RNA structural motifs on the influenza replication cycle.

INTRODUCTION

The influenza A virus causes a common respiratory disease that impacts a remarkable part of the human population in seasonal epidemic outbreaks and sporadic pandemics. The susceptibility of the virus to undergo genetic changes leads to the production of new strains, which may resist current therapeutic strategies.[1] To date, US Food and Drug Administration (FDA)-approved antivirals are directed at viral protein targets—neuraminidase (oseltamivir, zanamivir, and peramivir) and the M2 ion channel (amantadine and rimantadine).[2] Amino acid changes causing drug resistance were identified for both targeted proteins in some emerging influenza strains.[2] There is an urgent need to develop new approaches to viral inhibition. The influenza A virus genome consists of eight RNA segments, and the whole replication cycle is governed by the RNA and is dependent on its interplay and dynamics; thus, RNA is a good target for new therapeutics.[3,4] Published data show that influenza RNA has a complex secondary structure, and it is known and expected that RNA structure correlates with function.[5–22] To date, knowledge about the secondary structure of influenza RNA conserved motifs and entire segments has been successfully applied for the effective development of antisense oligonucleotides and triplex-forming peptide nucleic acid (PNA) oligomers.[12,14,15,22–24]

RNA-targeting strategies for the regulation of pathogenic RNA are still one of the most studied topics in novel therapy development. They include usage of antisense oligonucleotides, catalytic nucleic acids, and RNA interference (RNAi), as well as application of CRISPR/Cas technologies.[25,26] Undiscovered knowledge still limits our understanding and further application of each strategy.

One of the issues surrounding RNAi is the efficacy of small interfering RNA (siRNA) against different targets, which seems highly variable. A series of rules concerning duplex features were described and applied to improve siRNA design.[27] 21-nt siRNA carrying 2-nt 3′ overhangs were shown to be effective mediators of the RNAi. 2′-Deoxythymidine in the overhangs is favorable in terms of increased stability of the siRNA. The G/C content should be approximately 50% and G-rich sequences should be avoided. The nucleotide content analysis is especially important at the 5′ and 3′ ends where thermodynamic properties may determine siRNA duplex unwinding and guide strand selection. The siRNA sequence should be unique and target a single gene. Not much is known about target site requirements, especially within the scope of RNA structure. RNA hairpin stems as target regions have been reported to abolish RNAi, while hairpin destabilization influences RNAi in different ways without clear rules.[28,29] According to several studies, the target RNA structure may have inhibitory effects on RNAi efficiency, and therefore it is

Received 27 May 2019; accepted 16 December 2019;
https://doi.org/10.1016/j.omtn.2019.12.018.

Correspondence: Elzbieta Kierzek, Institute of Bioorganic Chemistry, Polish Academy of Sciences, Noskowskiego 12/14, 61-704 Poznan, Poland.
E-mail: elzbieta.kierzek@ibch.poznan.pl

reasonable to consider it in designing siRNAs. Some of the findings are still questionable due to contradictory results obtained by different research groups for both the siRNA and targets.[27–30]

In this study, we designed siRNAs targeting messenger RNA (mRNA) of segment 5 influenza virus (mRNA5) using additional structural criteria for selecting the RNA target region. The target site analyses were carried out on a secondary structure model of (+)RNA5 A/California/04/2009 (H1N1), predicted *in silico* based on bioinformatics data from *in vitro* mapping experiments and conservation of base pairs for type A influenza. We considered functionally important RNA secondary structure motifs and the RNAi structural accessibility for the potential targets. Segment 5 mRNA encodes nucleoprotein (NP). This structural protein is a part of all eight viral ribonucleoprotein (vRNP) complexes. It fulfils crucial roles in the viral replication cycle as a regulator of transcription, replication, and viral assembly.[3,4,31,32] NP is highly conserved among influenza A viruses, and it is probably also less prone to undergo changes causing drug resistance.[2] Influenza (−)RNA (vRNA) is used to produce two types of (+)RNA: cRNA (complementary RNA) and mRNA. The segment 5 mRNA differs from cRNA by being capped and polyadenylated. To date, segment 5 (+)RNA ((+)RNA5)) is the only influenza (+) RNA molecule for which a full-length RNA secondary structure has been determined and described in detail.[14] The published (+)RNA5 structure is based on a set of chemical mapping experiments and isoenergetic microarrays and is supported by bioinformatics analyses of more than 15,000 RNA sequences of type A influenza strains.[14] Therefore, it is possible to rationally design new siRNAs using a structural context for target sites. It is highly possible that previously identified conserved secondary structure motifs in the influenza A strains are preserved for certain functions, and therefore targeting them could influence viral replication. Twelve siRNAs targeting mRNA5 of strain A/California/04/2009 (H1N1) were designed and tested against influenza virus in Madin-Darby canine kidney (MDCK) cells. The results obtained herein demonstrate significant inhibition of viral replication and indicate that conserved structural motifs with accessible regions in RNA may serve as good targets for siRNA-mediated RNAi. Additionally, systematic studies of selected siRNAs with various modifications incorporated to improve siRNA inhibition were conducted. Twenty modified siRNA variants containing 2′-fluoro, thiophosphate, 2′-*O*-methyl, and DNA residues were synthesized, and their inhibitory properties were characterized showing that 2′-fluoro- and thiophosphate-modified siRNAs present the highest antiviral activity. Cell culture studies on modified siRNAs and antisense oligonucleotides targeting influenza RNA show the importance of the RNA target for selection of effective inhibitory oligonucleotide tools.

RESULTS

Design of siRNAs and ASOs Targeting Segment 5 mRNA

We selected the RNAi and antisense oligonucleotide (ASO) target regions based on the secondary structure of (+)RNA5 of the influenza A virus (Figure 1). The secondary structure of (+)RNA5 from A/California/04/2009 (H1N1) was folded based on the previously determined secondary structure of A/Vietnam/1203/2004 (H5N1) strain (+)RNA5, which is structurally conserved across type A influenza at an average of 87.6% of base pairs.[14] The secondary structure of (+)RNA5 of A/Vietnam/1203/2004 (H5N1) was proposed by applying experimental data, such as that obtained by chemical probing, isoenergetic microarray mapping, and sequence-structure bioinformatics analysis.[14] It was also previously shown that UTRs have minimal influence on global folding of (+)RNA5, and the majority of stable RNA motifs (except regions 577–593 and 833–931) fold independently from the 5′ and 3′ ends.[14] Such a secondary structure with a short distance of 5′ and 3′ ends is in agreement with observed and calculated universal properties of most mRNAs and also long non-coding RNAs (lncRNAs).[33] It is postulated that a short distance between mRNA ends could facilitate interactions of proteins and regulate translation regulation.[33] We therefore analyzed the (+) RNA5 secondary structure model as possessing important structural features that could exist in mRNA5.

Modeling of (+)RNA5 from A/California/04/2009 (H1N1) was conducted by comparison to the secondary structure of (+)RNA5 of A/Vietnam/1203/2004 (H5N1) using the Dynalign[34–36] mode of the RNAstructure 6.1 program by introducing conserved base pairs determined for type A ($\geq$99% conservation, Table S2) as folding constraints when submitting the A/Vietnam/1203/2004 (H5N1) (+) RNA5 sequence. Four out of 244 anticipated conserved base pairs (pairs 115–217, 133–165, 184–209, and 285–332) were excluded as constraints in prediction due to unfavorable free energy for formation of these base pairs in (+)RNA5 of strain A/California/04/2009 (H1N1) folding caused by the presence of neighboring unpaired nucleotides from both the 5′ and 3′ end (Figure 1; Table S2). A gap penalty of 0.4 kcal/mol was applied.

The preferential targets for ASOs or siRNAs were chosen in the (+) RNA5 structure regions that were highly modified by mapping reagents, structurally conserved, and potentially accessible for interaction with oligonucleotides (Figure 1). Additionally, siRNAs targeting mRNA5 were designed by RNAi Designer (Thermo Fisher Scientific), which fulfilled the general rules for selection of mRNA target sequences and requirements for effective interfering siRNA duplexes in mammalian cells (described in the Introduction).[27] The siRNA designing tool also confronts parameters of a proposed siRNA with the parameters and results obtained for known siRNA sets (tested on different target genes) to assess its potency. Both RNA target structure and sequence were considered in the final step. From the pool of molecules proposed by RNAi Designer, we chose nine siRNAs located in structurally predefined target regions (sequences in Table 1). Additionally, A/California/04/2009 (H1N1) sequence conservation among influenza type A strains in siRNA target regions was investigated (Table S3). The average sequence conservation ranged from 92.5% for the siRNA 183 target to 72.9% for the 1090 target. The highest average sequence conservation was calculated for positive control-siRNA 1498 (96.6%).

Positive and negative controls for the experiment were prepared. siRNA 1498 was used as a positive control and was derived from previously published results showing high inhibitory properties of

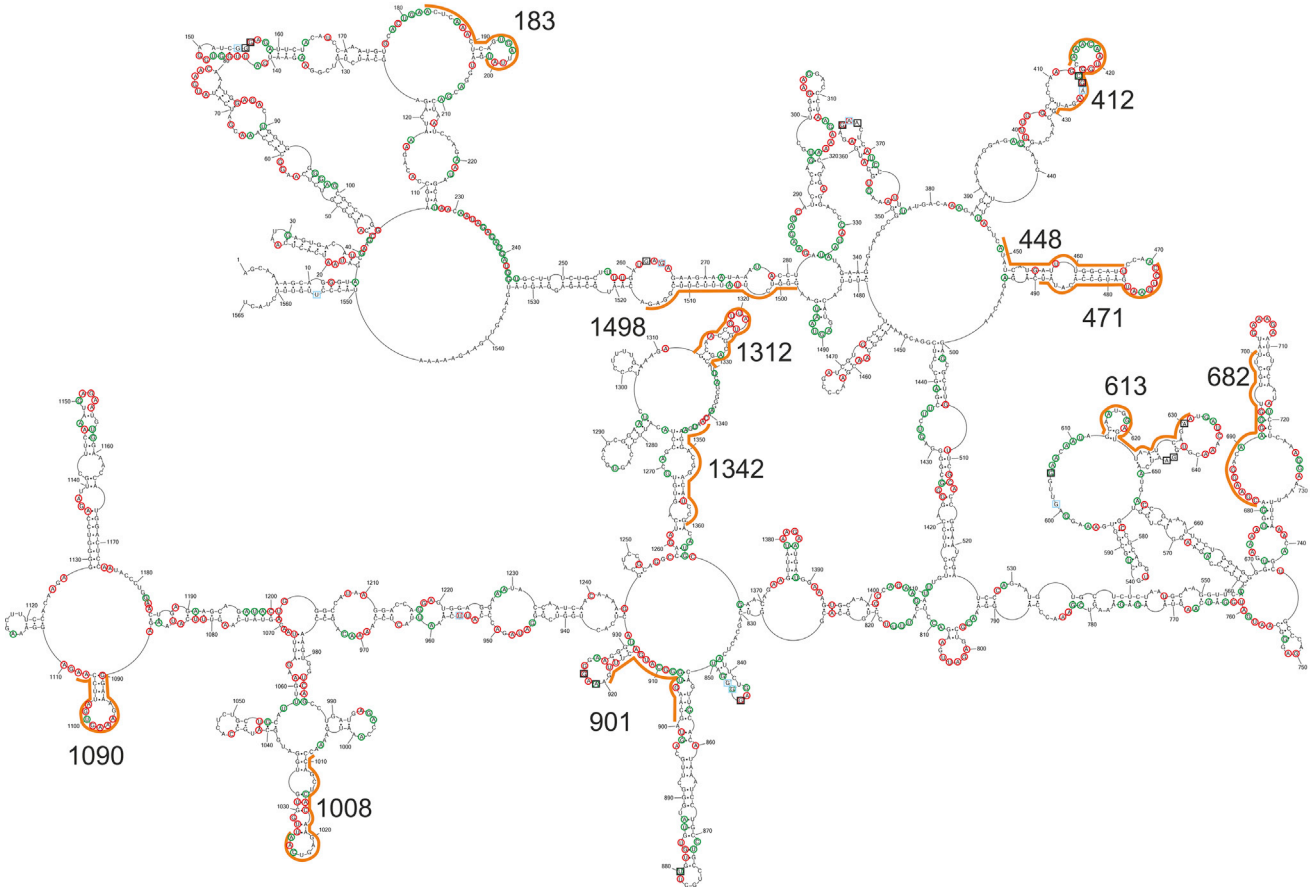

Figure 1. Self-Folding of (+)RNA5 A/California/04/2009 (H1N1) and siRNAs Target Regions

Secondary structure of (+)RNA5 A/California/04/2009 (H1N1) was predicted by Dynalign mode in RNAstructure 6.1 based on type A base pairs conservation data calculated from the previously determined (+)RNA5 secondary structure of A/Vietnam/1203/2004 (H5N1) strain. Target regions for designed siRNAs are marked with orange lines. For the RNA secondary structure model, the predicted accessible nucleotides are marked by a color-coded system based on reactiveness to chemical reagents, as well as isoenergetic microarray mapping results obtained for (+)RNA5 A/Vietnam/1203/2004 (H5N1). Symbols: red circles, predicted strong reactivity; green circles, medium reactivity; black squares, high accessibility to microarray probe; blue squares, moderate accessibility to microarray probe.

siRNAs targeting analogous regions of other H1N1 strains: A/PR/8/34 and A/WSN/33 (siRNA NP-1496), A/Beijing/01/2009 (NP-1494).[37,38] The negative control K1 was created by scrambling the sequence of one of the designed siRNAs, resulting in a sequence that was not complementary to either the viral or cellular sequences. In the study we also tested siRNAs 448 and 1342, which targeted less accessible regions (low content of reactive nucleotides in (+)RNA5 according to structural analysis) (Figure 1). The target region for siRNA 448 exhibits also a high average base pair conservation of 83.4%, while for 1342 it is 73%. All siRNA oligonucleotides were 21 nt long and synthesized with 2-nt TT overhangs at the 3′ end. For selected mRNA5 targets, ASOs were designed. ASOs were fully 2′-*O*-methylated RNA with locked nucleic acid (LNA) at selected positions to increase target binding and reduce the degradation rate.

Additionally, sequences of siRNAs 613, 682, 1312, and 1342 were adjusted for targeting A/PR/8/34 (H1N1) strain and named 613′, 682′, 1312′, and 1342′ (Table 1). The sequence identity between A/California/04/2009 (H1N1) and A/PR/8/34 (H1N1) strains for segment 5 coding sequence is 86%, which also implies changes in the siRNA sequences. Importantly, these sequence differences do not exclude base pairing of a target region that could be the same as in A/California/04/2009 (H1N1).

Inhibitory Potential of Unmodified siRNAs Targeting the A/California/04/2009 (H1N1) Segment 5 mRNA

Of the nine designed siRNAs, six inhibited influenza virus replication (Figure 2A). A concentration of 8 nM was sufficient to cause substantial antiviral effects. The most potent were siRNAs 613 and 682, which reduced viral copy number by 84.5% and 85.6%, respectively, in comparison with K1. Two other siRNAs, 1090 and 471, exhibited medium activity and inhibited influenza virus replication by 50.3% and 56.4%, respectively. Some of the siRNAs moderately influenced influenza virus proliferation. The reduction rate reached 42.3% for siRNA

Table 1. Sequences of Tested siRNAs and ASOs

Name	Sequence		Target Region
siRNAs			
1498	s1498	GGGUCUUAUUUCUUCGGAG**TT**	1498–1516
	a1498	CUCCGAAGAAAUAAGACCC**TT**	
1342	s1342	AAUGAAGGACGGACAUCCG**TT**	1342–1360
	a1342	CGGAUGUCCGUCCUUCAUU**TT**	
1342′	s1342′	A<u>C</u>AGA<u>G</u>GGA<u>A</u>G<u>A</u>ACAUC<u>U</u>G**TT**	
	a1342′	C<u>A</u>GAUGUU<u>C</u>UUCC<u>C</u>UC<u>UG</u>U**TT**	
1312	s1312	GCAACCGUUAUGGCAGCAU**TT**	1312–1330
	a1312	AUGCUGCCAUAACGGUUGC**TT**	
1312′	s1312′	<u>A</u>CAACC<u>A</u>UUAUGGCAGCAU**TT**	
	a1312′	AUGCUGCCAUAA<u>U</u>GGUUG<u>U</u>**TT**	
1090	s1090	GGAAAGAAAGUGAUUCCAA**TT**	1090–1108
	a1090	UUGGAAUCACUUUCUUUCC**TT**	
1008	s1008	CCCAGCUCACAAGAGUCAA**TT**	1008–1026
	a1008	UUGACUCUUGUGAGCUGGG**TT**	
901	s901	GCAAGUGGGCAUGACUUUG**TT**	901–919
	a901	CAAAGUCAUGCCCACUUGC**TT**	
682	s682	CGAAGGACAAGGGUUGCUU**TT**	682–700
	a682	AAGCAACCCUUGUCCUUCG**TT**	
682′	s682′	CGAA<u>AA</u>ACAAG<u>AA</u>UUGCUU**TT**	
	a682′	AAGCAA<u>UU</u>CUUGU<u>UU</u>UUCG**TT**	
613	s613	GCAAUGGAGUUAAUCAGAA**TT**	613–631
	a613	UUCUGAUUAACUCCAUUGC**TT**	
613-sF1	s613-sF1	G<u>fC</u>AA<u>fU</u>GGAG<u>fUfU</u>AA<u>fUfC</u>AGAA**TT**	
	a613	UUCUGAUUAACUCCAUUGC**TT**	
613-sF2	s613-sF2	G<u>fC</u>AA<u>fU</u>GGAG<u>fUfU</u>AA<u>fUfC</u>AGAA<u>fUfU</u>	
	a613	UUCUGAUUAACUCCAUUGC**TT**	
613-aF1	s613	GCAAUGGAGUUAAUCAGAA**TT**	
	a613-aF1	<u>fUfUfCfU</u>GA<u>fUfU</u>AA<u>fCfUfCfC</u>A<u>fUfU</u>G<u>fC</u>**TT**	
613-aF2	s613	GCAAUGGAGUUAAUCAGAA**TT**	
	a613-aF2	<u>fUfUfCfU</u>GA<u>fUfU</u>AA<u>fCfUfCfC</u>A<u>fUfU</u>G<u>fC</u>fUfU	
613-aF3	s613	GCAAUGGAGUUAAUCAGAA**TT**	
	a613-aF3	<u>fUfUfCfU</u>GA<u>fUfU</u>^{d}A^{d}A<u>fCfU</u>^{d}C<u>fC</u>A<u>fUfU</u>G<u>fC</u>**TT**	
613-asF1	s613-sF1	G<u>fC</u>AA<u>fU</u>GGAG<u>fUfU</u>AA<u>fUfC</u>AGAA**TT**	
	a613-aF1	<u>fUfUfCfU</u>GA<u>fUfU</u>AA<u>fCfUfCfC</u>A<u>fUfU</u>G<u>fC</u>**TT**	
613-sMe2	s613-sMe2	<u>G^{M}</u> <u>C^{M}</u> <u>A^{M}</u> <u>A^{M}</u> <u>U^{M}</u> GGAGUUAAUCAGAA**TT**	
	a613	UUCUGAUUAACUCCAUUGC**TT**	
613-sTT-PS	s613-sTT-PS	GCAAUGGAGUUAAUCAGAA<u>T^{PS}</u><u>T^{PS}</u>	
	a613	UUCUGAUUAACUCCAUUGC**TT**	
613-aTT-PS	s613	GCAAUGGAGUUAAUCAGAA**TT**	
	a613-aTT-PS	UUCUGAUUAACUCCAUUGC<u>T^{PS}</u><u>T^{PS}</u>	
613-sPS	s613-sPS	G<u>C^{PS}</u>AAUGGAGUUAAU<u>C^{PS}</u>AGAA**TT**	
	a613	UUCUGAUUAACUCCAUUGC**TT**	
613-aPS	s613	GCAAUGGAGUUAAUCAGAA**TT**	

(*Continued on next page*)

Table 1. *Continued*

Name	Sequence		Target Region
	a613-aPS	UU$\underline{C}^{PS}$UGAUUAA$\underline{C}^{PS}$U$\underline{C}^{PS}\underline{C}^{PS}$AUUG$\underline{C}^{PS}$TT	
613-asPS	s613-sPS	G$\underline{C}^{PS}$AAUGGAGUUAAU$\underline{C}^{PS}$AGAATT	
	a613-aPS	UU$\underline{C}^{PS}$UGAUUAA$\underline{C}^{PS}$U$\underline{C}^{PS}\underline{C}^{PS}$AUUG$\underline{C}^{PS}$TT	
613-sDNA	s613-sDNA	^{d}G^{d}C^{d}A^{d}AT^{d}G^{d}G^{d}A^{d}GTT^{d}A^{d}AT^{d}C^{d}A^{d}G^{d}A^{d}ATT	
	a613	UUCUGAUUAACUCCAUUGCTT	
613-aDNA	s613	GCAAUGGAGUUAAUCAGAATT	
	a613-aDNA	TT^{d}CT^{d}G^{d}ATT^{d}A^{d}A^{d}CT^{d}C^{d}C^{d}ATT^{d}G^{d}CTT	
613-siDNA	s613-sDNA	^{d}G^{d}C^{d}A^{d}AT^{d}G^{d}G^{d}A^{d}GTT^{d}A^{d}AT^{d}C^{d}A^{d}G^{d}A^{d}ATT	
	a613-aDNA	TT^{d}CT^{d}G^{d}ATT^{d}A^{d}A^{d}CT^{d}C^{d}C^{d}ATT^{d}G^{d}CTT	
613’	s613’	GUGAUGGAAUUGGUCAGGATT	
	a613’	UCCUGACCAAUUCCAUCACTT	
471	s471	CCUGAAUGAUGCCACAUAUTT	
	a471	AUAUGUGGCAUCAUUCAGGTT	
471-sF1	s471-sF1	fCfCfUGAAfUGAfUGfCfCAfCAfUAfUTT	
	a471	AUAUGUGGCAUCAUUCAGGTT	471–489
471-sF2	s471-sF2	CfCfUGAAfUGAfUGfCfCACAUAUTT	
	a471	AUAUGUGGCAUCAUUCAGGTT	
471-sMe1	s471-sMe1	C^{M} C^{M} U^{M} G^{M} A^{M} AUGAUGCCACAUAUTT	
	a471	AUAUGUGGCAUCAUUCAGGTT	
448	s448	CAUAUCAUGAUUUGGCAUUTT	448–466
	a448	AAUGCCAAAUCAUGAUAUGTT	
412	s412	GCAAACAAUGGCGAAGAUGTT	412–430
	a412	CAUCUUCGCCAUUGUUUGCTT	
183	s183	ACUCAAACUCAGUGAUUAUTT	
	a183	AUAAUCACUGAGUUUGAGUTT	
183-sF1	s183-sF1	AfCfUfCAAAfCfUfCAGfUGAfUfUAfUTT	183–201
	a183	AUAAUCACUGAGUUUGAGUTT	
183-sF2	s183-sF2	AfCfUfCAAAfCfUfCAGfUGAUUAUTT	
	a183	AUAAUCACUGAGUUUGAGUTT	
Negative control K1	sK1	GGUUUACCGUGUUCUGUGATT	–
	aK1	UCACAGAACACGGUAAACCTT	
Antisense Oligonucleotides			
682	AAG$\underline{C}^{L}$AA$\underline{C}^{L}$CCU$\underline{U}^{L}$GU$\underline{C}^{L}$CU$\underline{U}^{L}$CG		682–700
613	UU$\underline{C}^{L}$UGA$\underline{U}^{L}$UAA$\underline{C}^{L}$UC$\underline{C}^{L}$AU$\underline{U}^{L}$GC		613–631

The names of the siRNAs originate from the numbering of the first 5′ nucleotide at the (+)RNA5 target site (an “s” before the siRNA name means sense strand; an “a” means antisense strand). Modifications in the RNA sequence are marked with bold and underlined letters (**T**, thymidine residue; **fC**, 2′-fluorocytidine residue; **fU**, 2′-fluorouridine residue; $\underline{N}^{PS}$, phosphorothioate nucleotide residue; $\underline{N}^{M}$, 2′-*O*-methylated ribonucleotide residue; ^{d}**N**, deoxyribonucleotide residue, $\underline{N}^{L}$, LNA residue). Sequence changes in siRNAs targeting A/PR/8/34 (H1N1) are underlined (613′, 682′, 1312′, and 1342′). ASOs are fully 2′-*O*-methylated oligonucleotides.

183 and only 21.7% for siRNA 1312. siRNAs 412 and 1008 did not exhibit any inhibitory effect on influenza virus. siRNAs 448 and 1342, targeting RNA regions assigned as less accessible, showed low levels of viral RNA copy number reduction, that is, 28.2% and 21.1%, respectively. Interestingly, treating cell cultures with siRNA 901 led to significant enhancement of viral proliferation. The results obtained for siRNAs 613 and 682 were further confirmed in an immunofluorescence assay (IFA) assay (Figure 3). In both cases, virus titer was reduced compared to the negative control by 90.6% and 89.2% for siRNAs 613 and 682, respectively.

Next, we tested different concentrations of the most effective siRNAs—siRNAs 613 and 682—ranging from 100 to 2 nM. Increasing the concentration above 8 nM (50 and 100 nM) did not

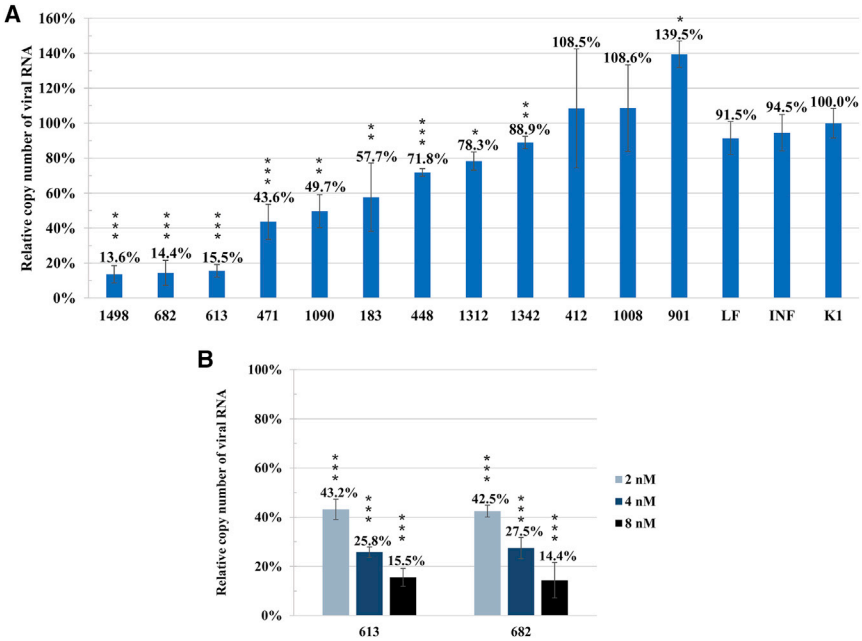

Figure 2. Inhibitory Potential of siRNAs against A/California/04/2009 (H1N1) in MDCK Cells

(A) Quantitative analysis of viral RNA by real-time PCR. RNA copy number of siRNA-treated samples at 8 nM concentration was compared to the RNA copy number of negative control K1 (established as 100%). (B) Graph of viral RNA copy numbers by real-time PCR for the most effective siRNAs tested at three concentrations. Cells treated with Lipofectamine 2000 without any siRNA are marked as LF; INF stands for untreated and infected cells. The error bars represent the standard deviations from three independent experiments. The unpaired two-tailed Student's t test was performed for statistical comparisons (*$p < 0.05$, **$p < 0.01$, ***$p < 0.001$).

yield superior inhibitory effects, and the viral RNA copy number remained at comparable levels. Decreasing the concentration from 8 nM to 4 or 2 nM caused proportional increases in the viral RNA copy number, demonstrating that antiviral activity of siRNAs is dose-dependent (Figure 2B). The 3-(4,5-dimethylthiazol-2-yl)-2,5-diphenyltetrazolium bromide (MTT) assay showed that the most potent siRNAs did not significantly affect cell viability, even at higher concentrations than routinely used in other published experiments (Figure 4).

The Effect of siRNAs 613′, 682′, 1312′, and 1342′ on Viral Proliferation Tested against A/PR/8/34 (H1N1) Strain

siRNAs 613′ and 682′ proved high inhibitory potential against A/PR/8/34 (H1N1) strain and reduced the viral RNA copy number by 85.3% and 78.0%, respectively (Figure 5). siRNAs 1312′ and 1342′ showed moderate antiviral activity, causing 19.3% and 17.3% inhibition of viral replication, respectively (Figure 5).

Modified siRNAs Design

Modifications were introduced into siRNAs 613, 471 and 183 according to previous reports,[39–42] and the modified siRNAs showed increased potential (sequences of all proposed siRNAs are presented in Table 1). The modified siRNAs fall into three distinct categories of antiviral activity—substantial, medium, and moderate. Full sets of 2′-fluorocytidine (fC) and 2′-fluorouridine (fU) nucleotides were incorporated into siRNA 613 in the sense and antisense strand (s613-sF1 and a613-aF1). Additionally, two variants of sense strands were prepared: one carrying 3′ TT overhangs (s613-sF1) and one with two 2′-fluorouridines at the 3′ overhangs (s613-sF2). There were also three variants of antisense strands (a613-aF1, a613-aF2, and a613-aF3). For the antisense strand variants, two (a613-aF1 and a613-aF2) were analogous to the sense strand, and the third had deoxyribonucleotides at positions 9, 10, and 13, which base pair with nucleotides lining the target cleavage site (a613-aF3, ending with 3′ TT overhangs). siRNAs 471 and 183 harbored full sets of modified cytidines and uridines in the sense strand (s471-sF1 and s183-sF1). There were also less modified variants of the sense strand, in which the alterations were concentrated at the 5′ region of the strand for both duplexes (s471-sF2 and s183-sF2).

As a second type of modification, we introduced thiophosphate residues to the sense and antisense strands of siRNA 613 (s613-sense phosphorothioate [sPS] and a613-aPS). These residues were located in the internucleotide bond following every cytidine. A similar modification pattern was applied for 2′-fluororibonucleotides; however, uridines were left unaltered. In contrast to 2′-fluororibonucleotides, incorporation of thiophosphates destabilizes the base pair in the duplex; therefore, excessive destabilization by extensive modifications was avoided.

2′-*O*-methylated siRNAs were also subjected to cell culture experiments. Sense strands of siRNAs 613 and 471 contained five modified nucleotides at their 5′ end (s613-sMe2 and s471-sMe1). Both strands of siRNA 613 were also synthesized as DNA variants (s613-sDNA and a613-aDNA). DNA:RNA hybrid siRNAs as well as DNA:DNA duplexes (often called siDNAs) were previously reported to inhibit viral RNA in mammalian cell culture.[43–45]

Antiviral Properties of Modified siRNAs Targeting Regions 183–201, 471–489, and 613–631

Experiments with 613-asF1 showed that a fully modified duplex with 2′-fluoropyrimidines results in a significant loss of siRNA antiviral potential. Furthermore, 2′-fluoro modification of the antisense strand without modification of the sense strand resulted in significant increases in the viral RNA copy number of 42.7%, 23.2%, and 52.1% for each tested variant (613-aF1, 613-aF2, and 613-aF3, respectively) compared to the unmodified duplex (Figure 6A). The presence of 2′-fluororibonucleotides only in the sense strand maintained a high level of viral inhibition (88.3% and 88.4% for 613-sF1 and 613-sF2,

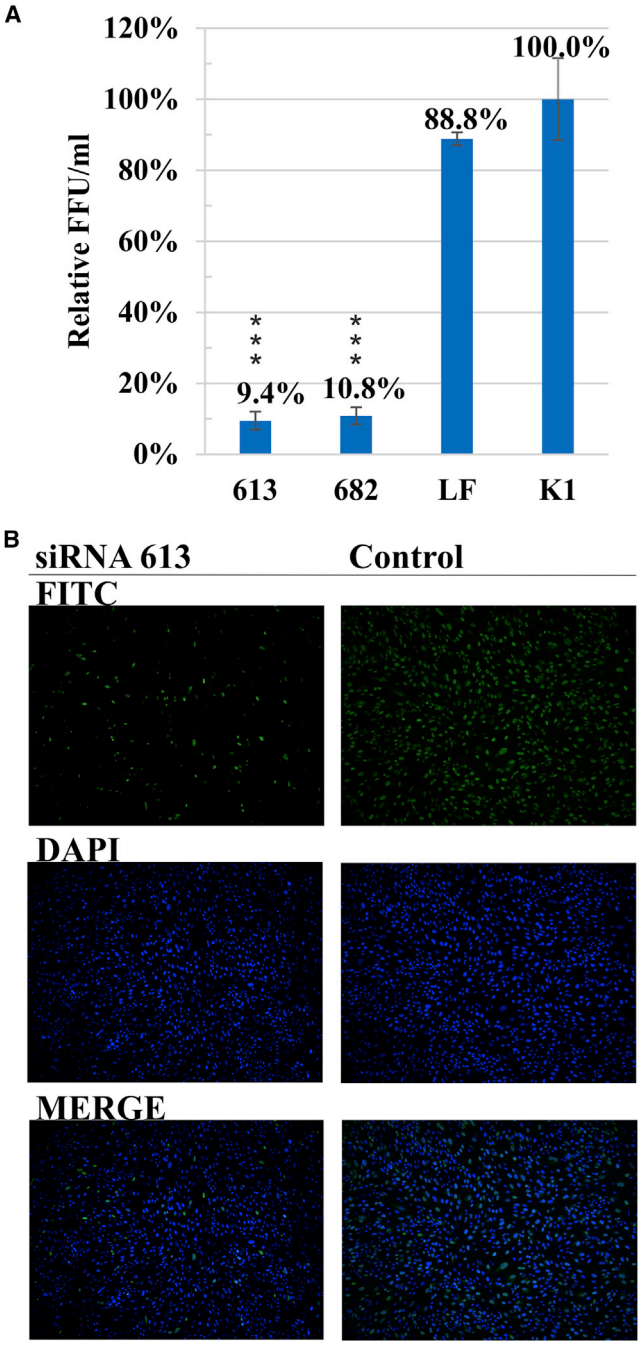

Figure 3. Antiviral Activity of the Two Most Effective Unmodified siRNAs Analyzed by IFA

(A) Results obtained for 8 nM siRNAs were compared to K1. LF is a Lipofectamine-treated control. The error bars represent the standard deviations from three independent experiments. The unpaired two-tailed Student's t test was performed for statistical comparisons (*$p < 0.05$, **$p < 0.01$, ***$p < 0.001$). (B) Exemplary fluorescence microscopy images of siRNA 613-treated cell culture and Lipofectamine control, infected with influenza virus in the IFA test. Green fluorescence is a FITC-conjugated secondary antibody targeting influenza NP protein; blue is nucleus DAPI staining. The signal from antibodies against the influenza NP protein is reduced in the sample treated with siRNA 613, demonstrating viral inhibition.

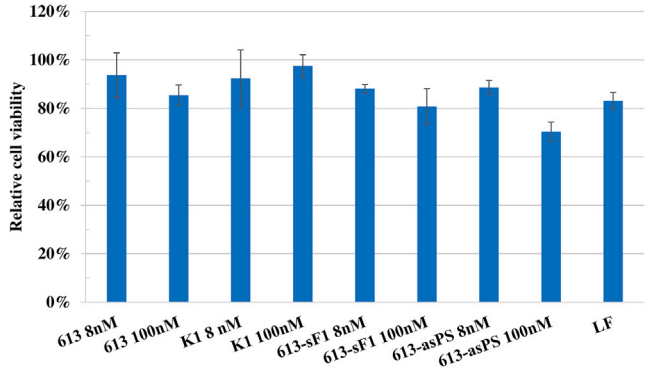

Figure 4. MTT Assay for the Most Effective Variants of siRNA 613 Performed at Various Concentrations

Cells treated with Lipofectamine 2000 without any siRNAs are marked as LF; the remaining labels are names of siRNAs. Cell viability of siRNA and Lipofectamine-treated samples was compared to untreated control established as 100%. The error bars represent the standard deviations from three independent experiments.

respectively). The results indicate that 2′-fluororibonucleotide substitutions are well tolerated in the sense strand, while they disrupt the effective RNAi process when placed in the antisense strand.

The situation was different in the case of siRNA 183 and 471 modifications. For 183-sF1, the viral RNA copy number increased by 22.4%, while 471-sF1 practically lost activity (Figure 6A). This result could be due to the number and distribution of modifications per sequence of oligonucleotide. 471-sF2 regained antiviral activity in the infected cell culture model comparable to that of the unmodified siRNA; however, no significant increase of inhibitory potential was observed. In the case of 183-sF2, the antiviral activity was higher than that of 183-sF1 but still lower than that of unmodified siRNA 183. Some differences may arise from modifications to the embedded cleavage site at 183-sF2 nucleotides 9 and 10. In 471-sF2, only one of the embedding nucleotides was modified.

In contrast, thiophosphates were well tolerated in both strands of siRNA. Introduction of this modification into one or both siRNA strands simultaneously had very similar inhibitory effects on influenza virus (Figure 6B). The analyses showed 77.9%, 80.2%, and 77.2% reductions of viral RNA copies in samples treated with duplexes in which modifications were distributed throughout the strands (613-aPS, 613-sPS, and 613-asPS, respectively). This result placed thiophosphate-modified siRNAs among the most active of the tested duplexes. However, when the 3′ TT overhangs were modified, the antiviral activity was diminished (613-aTT-PS and 613-sTT-PS). An inhibition of 58.3% was observed for siRNA with modified antisense strands and 67.6% for the modified sense strand. The negative influence of alteration was more prominent for the guide strand.

2′-*O*-methyl groups were introduced into the sense strand of siRNAs 613 and 471 at the 5′ ends (s613-sMe2 and s471-sMe1). Duplexes formed by nucleotides carrying 2′-*O*-methyl presented increased

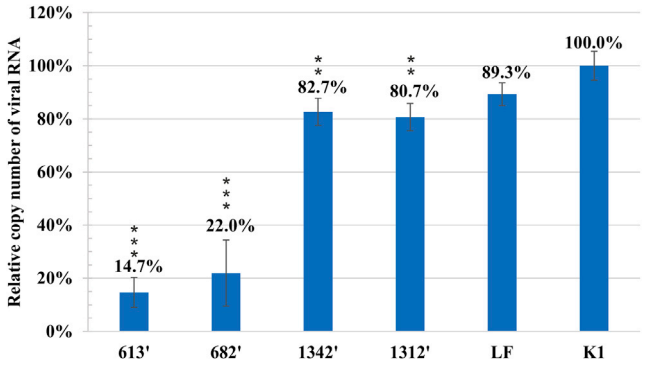

Figure 5. Inhibitory Potential of siRNAs 613′, 682, 1312′, and 1342′ against A/PR/8/34 (H1N1) in MDCK Cells

Quantitative analysis of viral RNA copy number by real-time PCR was carried out for siRNA-treated samples (8 nM) and compared to negative control K1 (established as 100%). LF is a Lipofectamine-treated control. The error bars represent the standard deviations from three independent experiments. The unpaired two-tailed Student's t test was performed for statistical comparisons (*p < 0.05, **p < 0.01, ***p < 0.001).

stability in previous studies.[39,42,46–48] Both modified siRNAs (471-sMe1 and 613-sMe2) reduced the inhibitory potential compared to unaltered variants, resulting in 30.9% and 60% reductions of viral RNA copies, respectively (Figure 6B).

Region 613–631 as a Target for DNA Interference

Both strands of siRNA targeting region 613 were converted into DNA sequences (s613-sDNA and a613-aDNA, Table 1). We tested 613-siDNA in cell culture and observed no reduction of RNA copy number (107.6% viral RNA copies) (Figure 6B). When the sense strand was made of RNA and the antisense strand DNA (613-aDNA), the results were very similar to the results evaluating the siDNA duplex (120.5% viral RNA copies). In contrast, when the inhibitory molecule consisted of a DNA sense strand and RNA antisense strand (613-sDNA), a substantial 68.1% viral inhibition was observed.

Inhibitory Activity of Antisense Oligonucleotides Targeting Regions 613–631 and 682–700

We also tested the 19-nt-long ASOs 613 and 682 (Table 1). Their sequences were equivalent to the siRNA 613 and 682 antisense strands with no 3′ TT overhangs. At the 8 nM concentration, which was the same concentration used for siRNA, neither ASO showed any antiviral activity. At a concentration of 750 nM, which has been used in previous experiments with ASOs targeting segment 5 (+)RNA, the viral RNA copy number was decreased by 26.9% and 26.8% for ASOs 613 and 682, respectively (Figure 7).

Serum Stability Assessment

Analyses indicate that the proposed modifications of the antisense strand of siRNA 613 and sense strand with 2′-fluororibonucleotides improve its serum stability (Figure 8A). After 2 h of incubation of siRNA 613 containing a modified antisense strand (613-aF1), almost the entire RNA pool remains intact. At the same time point, 60% of unmodified siRNA 613 is degraded. When the sense strand is modified (613-sF1), the siRNA stability is less pronounced. After 2 h of serum incubation, it exhibits approximately 80% integrity. siRNA with a thiophosphate-modified sense strand (613-sPS) did not exhibit improvements in serum stability, presenting stability comparable to that of the unmodified variant. The 2′-fluoro-modified sense strands of siRNAs 471-sF2 and 183-sF2 did not show enhanced stability. When comparing the stability of unmodified siRNAs, 471 and 183 are completely degraded during 2 h of serum incubation, while 40% of 613 remains intact.

Stability in Cell Lysates

Results indicate that the modifications (2′-fluororibonucleotides or internucleotide thiophosphates) introduced into siRNAs 613 (613-sF1, 613-aF1, 613-sPS, and 613-aPS) and 183 (183-sF2) improve stability of the duplexes in the cell lysates (Figure 8B). After 2 h of incubation more than 50% of the RNA pool remains intact. The most stable (almost 100% of intact siRNA) is 613-aPS. The unmodified siRNA 471 presents low stability in the cell lysate in comparison to siRNAs 613 and 183. 2′-Fluorosubstitutions in the sense strand of 471-sF2 do not improve this feature.

Thermodynamic Stability of siRNA and Modified siRNA

Thermodynamic parameters of unmodified siRNAs 613, 471, and 183 along with selected modified siRNA variants were measured (Table S4). Representative modified siRNAs were chosen to establish the influence of certain types of used modifications on siRNA stability. As expected, incorporation of 2′-fluoro modification in siRNA 613 slightly or moderately increases thermodynamic stability of duplex ($\Delta\Delta G^{\circ}_{37}$ = −4.52 kcal/mol for 613-sF, −1.57 kcal/mol for 613-aF1, and −4.48 kcal/mol for 613-asF1). PS modifications of siRNA 613 slightly increase thermodynamic stability of RNA duplex, with the stabilization effect ranging from −0.49 to −1.29 kcal/mol ($\Delta\Delta G^{\circ}_{37}$) for 613-aPS and 613-sPS, respectively, together with an insignificant change in the melting temperature. The effect of 2′-fluororibonucleotide incorporation in siRNAs 183 and 471 in slightly stabilizing or destabilizing duplex depends on modification positions. It is known from systematic studies that 2′-*O*-methylation stabilizes RNA/RNA duplexes, and 2′-*O*-methyl (2′-OMe)-RNA/RNA has increased thermodynamic stability versus RNA/RNA.[49] Surprisingly, 471-sMe1 and 613-sMe2 showed much lower thermodynamic stability than did parent unmodified siRNAs ($\Delta\Delta G^{\circ}_{37}$ = 12.22 and 10.37 kcal/mol for 471-sMe1 and 613-sMe2, respectively). This observation could be connected with partial and unsymmetrical stabilization of one siRNA side of duplex, although analysis of the measurement data showed two-state melting.

DISCUSSION

Conserved RNA Secondary Structure Motifs Are Good Targets for RNAi

For the first time, we modeled the secondary structure of (+)RNA5 of A/California/04/2009 (H1N1) by using available experimental and bioinformatics data, as well as selected targets for siRNAs and ASOs (Figure 1). Such *in vitro* RNA structure determinations appear to be valuable for consideration of accessible targets within conserved-for-type A structural motifs that could exist at a certain

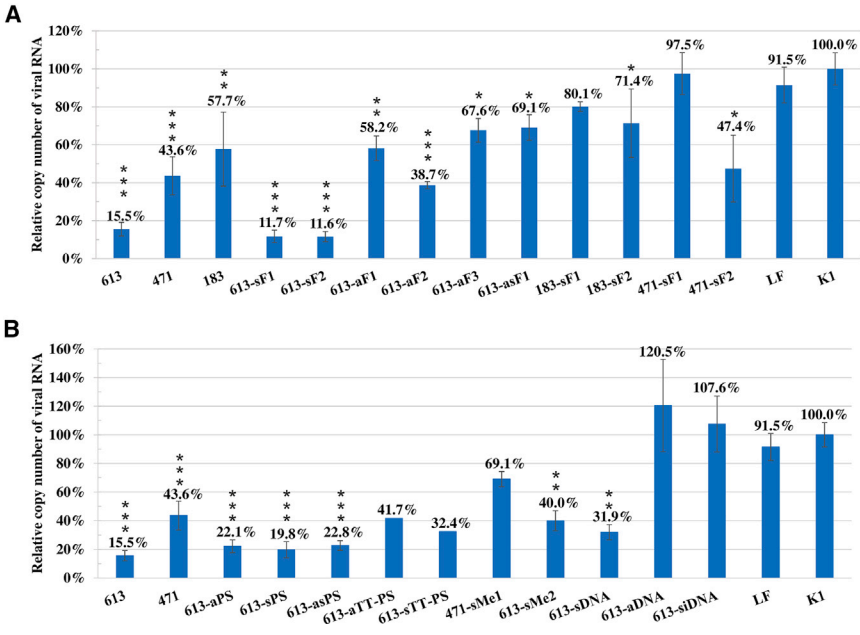

Figure 6. Inhibitory Potential of Modified siRNAs at 8 nM Concentration against A/California/04/2009 (H1N1) in MDCK Cells

(A and B) Quantitative analysis of viral RNA copy number performed by real-time PCR for (A) siRNAs containing 2′-fluororibonucleotides and (B) siRNAs modified with thiophosphates, 2′-*O*-methyl-siRNAs, and siDNA. Cells treated with Lipofectamine 2000 without any siRNA are marked as LF. The error bars represent the standard deviations from three independent experiments. The unpaired two-tailed Student's t test was performed for statistical comparisons (*$p < 0.05$, **$p < 0.01$, ***$p < 0.001$).

stage of the viral cycle. The knowledge on influenza RNA secondary structures *in vivo* is very limited and hard to interpret. The first report concerning influenza mRNA structure, obtained from dimethyl sulfate (DMS) mapping of preinfected, snap-frozen cell culture pellets, was recently published.[21] It confirmed the presence of several stable local structural motifs in mRNA5 of A/Puerto Rico/8/1934 (H1N1) strain. However, it also revealed many regions with high A and C reactivity to DMS, predicted as unfolded. Direct information on potential and important structure changes at different stages of infection and the viral replication cycle is still missing. Especially for other viral RNAs, the structure of *in vivo* dynamics was already recognized.[50] Therefore, the presented approach deals with this gap and leads to the design of inhibitory siRNAs. The approach takes advantage of the fact that despite frequently occurring changes in viral RNA sequences, the functional secondary structures are still preserved. Bioinformatics sequence-structure analysis supported by experimental *in vitro* data could be a powerful method for identification of siRNA targets.

Among the tested siRNAs, the most potent are siRNAs 613 and 682 (Figure 2). siRNA 613 partially overlaps the binding site in hairpin loops of previously tested ASOs 615A and 640A, which effectively inhibit virus proliferation (70% and 64% reduction, respectively, of viral RNA copy number in real-time PCR analysis).[14] These neighboring regions as targets for two different RNA-directed strategies support the idea that certain stable and conserved motifs are functionally significant. Additionally, results concerning siRNAs 448 and 1342 targeting less accessible RNA regions (Figure 1), and serving as negative controls, show minimal reduction of viral replication. These findings suggest that analysis of target RNA structure may be applied as an indicator of good targets as well as regions less potent or not suitable for efficient inhibition.

Region 591–612 nt adjoining the siRNA 613 target site was targeted by effective siRNAs published by other research groups (NP571 and NP574).[38] At 40 nM, NP571 and NP574 caused an approximately 80% reduction in NP mRNA and approximately 70% protein reduction for strain A/Beijing/01/2009 (H1N1). Region 649–667 nt, which is separated from the siRNA 613 target site by 17 nt, was targeted previously by NP604 (siRNA generated in cells from the plasmid construct), causing inhibition of strain A/duck/Fujian/13/2002 (H5N1) proliferation.[51] Although the experiments were conducted on different strains and the inhibitory effects were monitored by different methods, it is clear that the targeted structural domain is functionally important and prone to siRNA-mediated inhibition of influenza replication.

The second siRNA, 682, targeted a partially single-stranded region localized on the opposite site of a long internal loop that is a binding site for inhibitory ASO 727A (target region: 722–732 nt) that was previously tested.[14] This result indicates that the structural motif 671–743 may fulfill an especially important role in the viral life cycle, and this motif is disrupted by RNA-targeting strategies. Interestingly, siRNAs 471, 1312, and 183 have overlapping binding sites with previously tested ASOs 470A, 1320A, and 200A (target regions: 466–478, 1308–1328, and 194–206 nt, respectively) and showed medium to moderate activity in proliferation inhibition, while the ASOs were not able to inhibit virus (Figure 2A).[14] siRNAs 412 and 901 had partially overlapping target sites with ASOs 415A and 920A (target regions: 410–426 and 917–929 nt, respectively) and did not exhibit antiviral properties (Figure 2A), which was consistent with the results obtained for ASOs.[14] The ASOs and siRNAs were used at different concentrations of 8 and 750 nM, respectively.

The two strategies presented using siRNA and ASO proceed through different pathways. The role of RNA structure in the RNAi process is still not fully understood. The fact that the target sites for effective ASOs are also favorable for siRNA activity indicates that the structure-based design of molecules is a reasonable way to improve effective siRNA design. The presented approach also provides some new insights into the biology of the influenza virus. We assume that target

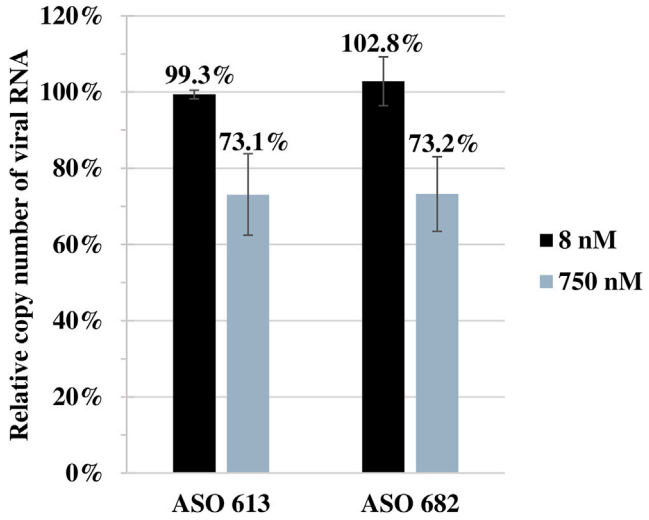

Figure 7. Antiviral Activity of ASOs against A/California/04/2009 (H1N1) in MDCK Cells

Quantitative real-time PCR analysis of RNA copy number in ASO-treated samples at two concentrations was compared to the viral RNA copy number of Lipofectamine-treated cells established as 100%. The error bars represent the standard deviations from three independent experiments.

regions of the best siRNAs are especially important for the viral life cycle and may carry a functional role.

The RNA regions targeted by the most potent siRNAs, 613 and 682, against A/California/04/2009 (H1N1) are also powerful targets in A/PR/8/34 (H1N1) (siRNAs 613′ and 682′) in this study. Similar inhibition rates using both siRNAs were observed in the cell culture for both strains (Figures 2A and 5). Analogous results were obtained for siRNAs with low potential to reduce influenza virus titer (1312 and 1312′, 1342 and 1342′). These results may indicate that, despite the sequence differences between strains, the structure and function of the RNA domains are preserved. siRNAs 1312 and 1342 as well as 1312′ and 1342′ targeted less accessible regions in *in vitro* (+)RNA5 secondary structure and, as expected, all insignificantly lowered virus replication. Interestingly, the observed inhibition for 1312′ did not correlate with an accessible hairpin loop in the motif proposed for these regions from *in cellulo* studies of A/PR/8/34 (H1N1).[21] The sequence identity in the coding region of segment 5 for A/California/04/2009 (H1N1) and A/PR/8/34 (H1N1) (86%) is advantageous for investigating structure conservation. The structure and function conservation between strains may give a foundation to siRNA design directed at predefined, important RNA motifs, but also taking into account sequence changes.

The highest inhibitory effects of siRNAs 613 and 682 were achieved with a low concentration of 8 nM. It was shown previously that Eri-1 intracellular exonuclease, which is a negative regulator of RNAi, was upregulated in response to high doses of siRNA.[40] It is more appropriate to use lower doses of siRNAs in some cases. The siRNAs show high antiviral activity at relatively low concentrations, which prevents excessive activation of siRNA negative regulators. Reducing the effective concentration is also a favorable feature when siRNA is considered as a potential therapeutic strategy, since it is associated with minimization of both toxicity and costs.

In previous publications concerning anti-influenza siRNA evaluation in animal models, a few approaches of nucleic acid delivery were applied. Influenza virus infections include the upper respiratory tract, and inhalation is one of the possible routes to directly deliver inhibitory molecules to the area of infection.[52–54] The second route is intravenous injection, which was also successfully tested.[53–58] The siRNAs may be used as short duplexes or as shRNA vectors. In both cases, naked nucleic acids, liposomal formulations, or polymer carriers were administered. Additionally, polyethyleneimine (PEI) was reported to promote lung tissue localization after intravenous injection.[54] The abovementioned methods could be also considered for further *in vivo* studies in animal models for siRNAs presented herein. Simultaneously, research on new carriers, e.g., nanoparticles and tissue-targeting moieties, is underway, which may improve nucleic acid delivery and membrane penetration in the future.[59]

Chemical Modifications Influence siRNA Activity against Influenza Virus

Chemical modifications are widely applied in antisense strategies to increase the stability of oligonucleotides, provide resistance to nucleases, improve target binding, reduce off-target effects, and prolong activity.[60] Modifications of siRNA may influence different stages of RNA-induced silencing complex (RISC) actions, such as recognition, loading, and helicase activity, due to H-bond, and electronic and steric effects.[40,61] The main aim is to find modifications that facilitate desired specific effects, increase the plasma stability, and maintain low cytotoxicity of the siRNA.

2′-Fluororibonucleotides Are Well Tolerated in the siRNA 613 Sense Strand

Some of the previous publications indicated that 2′-fluororibonucleotide modifications in the antisense strand are more tolerated at the 3′ end and retain the ability of siRNA to silence genes.[39] Excessive modification of the 5′ end in the antisense strands proposed by us may have contributed to the reduced activity of 613-aF1, 613-aF2, 613-aF3, and 613-asF1 (Figure 6A).

Sequence-dependent composition of siRNA (every C and U modified in the strand) determined the number of changes in the strands. siRNA activity was unaffected when the level of modification in the sense strand was moderate (613-sF1 and 613-sF2; Figure 6A). RNAi activity was reduced when the sense strand was heavily modified (471-sF1 and 183-sF2; Figure 6A). Limiting the level of modification in this case improved inhibition (471-sF2 and 183-sF2; Figure 6A).

Excessive modification with stabilizing groups (2,6-diaminopurine, 2′-fluoro, 5-bromouridine, and 5-ioidouridine) was shown to be disadvantageous for RNAi in previous studies.[39] The factor responsible for

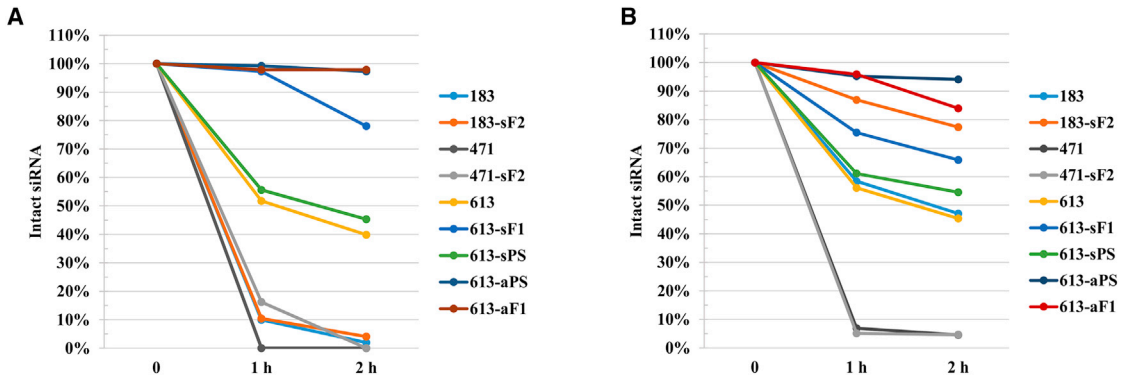

Figure 8. Stability of Selected siRNA Variants

(A and B) Integrity of siRNA was analyzed in serum (A) and cell lysates (B) at three time points and compared to the sample collected right after dissolving in the FBS solution or cell lysate (established as 100%), respectively.

the limited potential of excessively modified siRNA may be impaired recognition by the RISC complex due to introduction of modified nucleotides. It was previously shown that the RISC RNA-binding domain binds different sequences and nucleotides with variable affinity.[62,63] These studies did not include modified nucleotides, and the exact mechanisms governing the RNA-protein interaction are still unknown. The disruption of antisense strand interaction with RISC (by excessive modification) might cause reduced activity of siRNA 613-aF1, 613-aF2, 613-aF3, and 613-asF1 (Figure 6A). The antisense strands of these siRNAs contained more nucleotide substitutions (12–15) than did highly active siRNAs 613-sF1 (6) and 613-sF2 (8) with 2′-fluoro-modified sense strands.

It is still unclear how certain modifications affect cleavage event that occur during RNAi. According to previous reports, the presence of 2′-OH is not required for RNAi for nucleotides of the antisense strand pairing with mRNA cleavage site.[39] We also have limited knowledge of how modifications influence passenger strand fate after separation of the siRNA strands. Lack of cleavage in the sense strand between nucleotide 9 and 10 was previously reported to impair RNAi.[40] We designed siRNAs in which the distribution of 2′-fluorocytidine and 2′-fluorouridine was even, with no cleavage site exception. The most effective modified siRNAs in our studies—613-sF1 and 613-sF2—contained one modification at the cleavage site. This observation may indicate that the lack of 2′-OH in this position does not disturb siRNA activity.

siRNAs modified with 2′-fluorocytidine and 2′-fluorouridine were previously shown to successfully silence targeted genes.[39,40] These observations were generally consistent with our results. It was also previously reported that modification of sense strands could be favorable for siRNA activity, as it protects the guide strand to retain its integrity at stages preceding RISC activation.[40] The reports about increased thermal stability of 2′-fluoro-modified duplexes are consistent with our UV melting results obtained for siRNAs 613-aF1, 613-sF1, and 613-asF1 (Table S4). 2′-Fluororibonucleotide modifications were described to protect siRNAs against intracellular RNases (especially Eri-1 exonuclease that negatively regulates RNAi) and enable extended activity within the cells. Finding suitable siRNA modification patterns even for a single duplex may lead to improvements that will be beneficial for future applications.

Moderate Level of PSs in siRNA Does Not Disturb RNAi

In our studies, PSs were well tolerated in both the sense and antisense strands of siRNA 613 when distributed throughout the RNA strands. siRNAs maintained high antiviral activity despite different localization and numbers of modifications in both strands (613-sPS, 613-aPS, and 613-asPS, Figure 6B).

It was previously reported that incorporation of this modification has less influence on siRNA activity when introduced only to the sense strand.[39] However, duplexes containing fully modified sense strands were significantly less effective than unmodified duplexes in previous studies.[41] Our data show that there is no remarkable difference in the inhibitory effect between samples treated with siRNA containing PS linkages and the unmodified variant at low concentrations used for cell culture experiments (8 nM). Additionally, the reduced inhibitory effect caused by the incorporation of PS linkages at the 3′ ends for both siRNA strands (613-aTT-PS and 613-sTT-PS) is contrary to previous findings, in which no significant loss of silencing efficacy was noted.[42] Our results support a crucial role of the siRNA 3′ end in RISC binding, which may be disturbed by modifications.[62]

From the future application point of view, PS modification carries some favorable features. Similar to 2′-fluororibonucleotides, PS modifications increase the half-life of siRNAs exposed to cytoplasmic extracts or serum. PS linkages in oligonucleotides administered *in vivo* increase binding to serum proteins, the level of clearance from the organism is lower and tissue bioavailability is improved.[41,47,64]

Adverse Effects of 2′-*O*-Methylation on siRNA activity

2′-OMe modification of RNA is known to increase its chemical stability and prevent degradation by enzymes, increase affinity for RNA

targets, and increase thermodynamic stability of the duplex with RNA.[42,49,61,64] It was also postulated that siRNA sense strand modifications may eliminate off-target effects due to preferential antisense strand selection by the RISC complex.[65] Unfortunately, in this study, incorporation of five 2′-OMe nucleotides at the 5′ end of the siRNA sense strand led to a substantial decrease in silencing efficacy (471-sMe1 and 613-sMe2, Figure 6B).

Some of the previously designed 2′-OMe-modified siRNAs showed increased serum stability and retained knockdown efficiency.[42,48,61] However, diminished or completely abolished RNAi was also observed in those experiments.[39,42] In these publications, the authors investigated many siRNA variants, and the results did not point to any unambiguous modification pattern. The loss of activity was blamed on the bulky size of the methyl group. This feature may negatively influence interactions between siRNAs, target mRNAs, and the RISC complex. Such effects could influence the activity of 2′-*O*-methylated siRNAs tested in this study and cause diminished antiviral potency. In particular, the uneven distribution and accumulation of the modified residues at the 5′ end may have led to the failure of the approach. Moreover, previous studies revealed that the disruption of gene silencing by modifications depends on the size of the modifying groups: the larger is the group, the stronger is the activity reduction.[65] This finding corresponds with our other results, in which 2′-fluoro groups, causing the most subtle steric hindrance, allow silencing at comparable levels to those of unmodified siRNA. Conversely, a large size of the methyl group significantly disturbs the silencing process.

Application of siDNA Was Not Effective When Targeting mRNA5 Region 613–631, whereas Hybrid 613-sDNA Inhibited Viral Replication

It was previously shown that siRNA tolerated some level of DNA substitution.[39] In some studies, pure RNA-DNA hybrids were unable to induce RNAi probably due to their structure, which is an intermediate between an α and β helix.[66] These observations are not fully consistent with other reports showing that the DNA interference phenomenon may occur within cultured human cells.[43–45] Although DNA interference was first described in plants, it is currently known that siDNAs are able to inhibit viral RNA in mammalian cell culture.[43] These findings are supported by crystallographic studies of Ago PAZ domains demonstrating their ability to bind DNA.[67] In our studies, siDNA was not able to inhibit influenza virus RNA in MDCK cells (613-siDNA, Figure 6B). Conversely, the RNA-DNA hybrid 613-sDNA showed significant levels of antiviral activity (Figure 6B). It was necessary to leave the RNA antisense strand unaltered to obtain inhibition.

Published studies concerning posttranscriptional gene silencing indicate possible pathways for this process.[39,68,69] The cellular machinery used for the abovementioned silencing is mostly the same as for siRNA-mediated RNAi. In the process guided by microRNA (miRNA), there is no degradation step and an α helix is not required for activity. It seems that only RNA degradation is helix-dependent. This should be considered when analyzing results obtained for our RNA-DNA hybrids, in which the sense strand was DNA and the duplex retained some degree of inhibition. A possible explanation is that the hybrid was recognized by the RISC complex and the antisense RNA strand could act as a conventional siRNA. In the view of contradictory published data, the exact pathway is still unclear.

siRNAs Are Shown to Have Superior Antiviral Potential Compared to ASOs When Targeting the Same mRNA5 Regions: 613–631 and 682–700

ASOs with sequences equivalent to the guide strand of the most potent siRNAs in this study did not exhibit significant antiviral potential (Figure 7). The concentration needed to obtain any inhibitory effect was much higher than that for the siRNAs: 750 nM for ASOs 613 and 682 and less than 8 nM for siRNAs 613 and 682 (Figure 2A). Even at high concentrations, the inhibition was low (27%) in comparison to siRNAs (85%). The target region of ASO 613 partially overlaps with the target region for previously tested ASOs that presented high antiviral potency. The shifts result in the activity loss. This may be due to the structural context of the target. ASOs 615A and 640A were designed to target mostly single-stranded regions. The ASO 613- and 682-target regions are partially double stranded. Accessibility of regions involved in secondary structure may limit the interactions needed for inhibition. Our experimental data indicate that regions selected as good targets for RNAi may not be susceptible and accessible for the conventional antisense strategy. The fundamental factor determining this process may be the different molecular processes induced by these two types of approaches. RNAi seems to be more flexible in terms of target structure selection in comparison to ASOs, but other rules regarding target sequence apply.

Increased Stability of siRNAs Cannot Be Assured by All Modifications

The majority of unmodified siRNAs are degraded within 20 min, and nearly complete degradation is observed by 3 h in 10% serum.[70] Note that during transfection, siRNAs are protected by the lipid shell of the carrier, and a direct exposure to serum does not occur at this stage of cell culture experiments. Then, after penetrating the cell membrane, siRNAs are exposed to intracellular RNases. In serum stability tests, we observed that 2′-fluororibonucleotides and thiophosphates introduced into siRNA strands may improve their properties (613-sF1, 613-aF1, and 613-aPS; Figure 8A). Some of the tested siRNAs were more stable in the cell lysates than in the serum (183 and 183-sF2) (Figure 8B). These differences may arise from varied composition of extracellular and intracellular fluids. Nevertheless, modification may have an important impact on siRNA stability. For siRNA 613, a few variants of a modified sequence were tested. In both experiments (stability in serum and cell lysates) the level of stability was dependent on the number of modified nucleotides in the siRNA 613 strand.

It was previously postulated that there is a direct link between duration of the RNAi effect and siRNA stability in human cells.[39] Serum stability is also an important factor when considering future

applications of siRNA, especially intravenous administration. The level of modification should be considered. Interestingly, the most stable unmodified and modified duplex is the most active in terms of inhibitory properties (siRNA 613).

Conclusions

Applying knowledge of RNA secondary structures as additional criteria in designing siRNAs appears to be a promising approach. siRNAs selected this way were effective against influenza virus molecules at low concentrations. Additionally, our research identified regions that were both accessible for RNAi machinery targets in the mRNA5 and significantly reduced viral replication of influenza virus type A. Notably, the best RNA target regions for the oligonucleotide-based strategies could be different for siRNAs and ASOs. Finding favorable modification patterns for siRNAs is challenging. We observed that one type of modification may have adverse effects on the activity of different siRNAs depending on the position of the modification in the siRNA and RNA targets. Additionally, the results obtained for one type of modification cannot serve as a simple template to predict siRNA activity with other kinds of modifications. Determining a good target for unmodified siRNA in mRNA5 and applying different types of modifications in systematic studies allowed us to develop siRNAs with improved inhibitory effects against influenza virus type A.

MATERIALS AND METHODS

Cell Culture and Virus Titration

MDCK cells (Sigma) were cultured in Dulbecco's modified Eagle's medium (DMEM; Gibco) supplemented with 10% heat-inactivated fetal bovine serum (FBS, Gibco), 2 mM glutamine, and penicillin (100 U/mL) and streptomycin (100 μg/mL) (penicillin-streptomycin-glutamine [100×]; Gibco) in 5% CO_2 at 37°C. Experiments were carried out on the A/California/04/2009 (H1N1) (a gift from Prof. Luis Martinez-Sobrido, University of Rochester) and A/PR/8/34 (H1N1) influenza strains propagated in MDCK cells. The virus titer was determined by a standard plaque assay.[14]

Synthesis and Deprotection of the Oligonucleotides

Primers for PCR, real-time PCR, and reverse transcription, as well as ASOs and siRNAs (Table 1; Table S1), were synthesized by the phosphoramidite approach on a MerMade 12 (BioAutomation) RNA/DNA synthesizer. Natural and modified phosphoramidites as well as supports were purchased from ChemGenes and GenePharma. Oligonucleotides were deprotected and purified according to published protocols.[71–73] Real-time PCR probes were synthesized with 5-carboxyfluorescein (5-FAM) at the 5′ end and an amino-linker at the 3′ end. After deprotection and desalting, the probes were labeled at the 5′ end with 6-carboxytetramethylrhodamine (6-TAMRA) (AnaSpec) and purified as described before.[14]

siRNA and Oligonucleotide Transfection

Transfection of siRNAs and ASOs into the cells was carried out using Lipofectamine 2000 (Invitrogen). Lipofectamine 2000 was diluted 36.5-fold in Opti-MEM (Invitrogen) and incubated for 10 min at room temperature (RT). Next, siRNA or ASO was diluted with Opti-MEM, and 33.5 μL of the solution was mixed gently with 100.5 μL of Lipofectamine-Opti-MEM solution and incubated for 30 min at RT. In general, the final concentration of siRNA during transfection was 8 nM. For dose-dependency studies, we also tested 100, 50, 16, 4, and 2 nM concentrations of siRNAs. ASOs were transfected at 8 and 750 nM. Just before the transfection, MDCK cells were trypsinized and resuspended in fresh culture medium. Transfection solution was added to the MDCK cell suspension containing 1.2×10^5 cells per well at a final volume of 670 μL, which was seeded in 24-well plates. After 12 h of incubation, the transfection medium was replaced with standard culture media.

Influenza Virus Infection

Eighteen hours after transfection, the cell cultures were washed with PBS and infected with influenza virus A/California/04/2009 (H1N1) or A/PR/8/34 (H1N1) at an MOI of 0.01. The cells were incubated with a solution containing virus diluted with infection medium (0.3% BSA [Sigma] and 100 U/mL penicillin/100 μg/mL streptomycin [penicillin-streptomycin; Sigma] in PBS) for 1 h at RT on a gently rocking platform. The supernatant was then removed, and the cells were maintained in postinfection medium (0.3% BSA, 100 U/mL penicillin, 100 μg/mL streptomycin, 2 mM glutamine, 1 μg/mL N-tosyl-L-phenylalanine chloromethyl ketone [TPCK]-treated trypsin [Sigma] in DMEM) at 33°C for 24 h.

Virus Quantitative Real-Time PCR Analysis

Total RNA from the cell monolayer was extracted using TRIzol reagent.[74] Five hundred nanograms of each isolated sample was treated with RNase-free DNase I (0.1 U/μL; Invitrogen) in 1× DNase I buffer in a 10-μL reaction at 37°C for 30 min. Enzyme inactivation was performed by adding 1 μL of 25 mM EDTA to reach a final concentration of 2.3 mM and heating at 75°C for 10 min. Agarose gel electrophoresis was conducted to check the quality of isolated RNA. Reverse transcription was performed with gene-specific primers complementary to the vRNA7 sequence[75,76] (Table S1) and SuperScript III reverse transcriptase (Invitrogen). One microliter of sample from the DNase I treatment was mixed with 1× first-strand buffer, 0.4 μM gene-specific primers, and H_2O to bring the volume to 5 μL. The mixture was incubated for 3 min at 90°C, 10 min at 55°C, and then placed on ice. Then, 10 mM DTT, 2.5 mM 2′-deoxynucleoside 5′-triphosphates (dNTPs), 1× first-strand buffer, 10 U of RNasin inhibitor (Promega), and 50 U of SuperScript III reverse transcriptase were added to the final volume of 10 μL and incubated for 50 min at 55°C. The reaction was inactivated by heating at 70°C for 15 min. One microliter of the obtained cDNA was subjected to real-time PCR with gene-specific primers (Table S1) and 5× HOT FIREPol Probe qPCR Mix Plus (Solis BioDyne) according to the manufacturer's protocol. Real-time PCR absolute quantification of viral RNA allowed for the determination and comparison of viral RNA copies in distinct samples. The viral RNA copy number for each siRNA-treated sample was calculated as a percentage of viral copy number detected in the negative control, which was established as 100% of the viral RNA copies. The assays and analyses were performed simultaneously, and the data have been divided into several figures for better comparison and interpretation.

Indirect IFA

Supernatants collected from infected cell culture were used to prepare 10-fold serial dilutions of the virus with infection medium. Cell culture monolayers in 96-well plates were infected with serial dilutions of viral supernatants for 1 h at RT on a gently rocking platform. Then, supernatants were discarded and cells were maintained in post-infection medium for 8–10 h at 33°C and 5% CO_2. The supernatants were again removed, and the cells were fixed and permeabilized with 4% formaldehyde and 0.5% Triton X-100 solution (BioShop) in PBS for 20 min at RT. Blocking was performed using 3% BSA solution in PBS for 1 h at RT. Next, the solution was replaced with the mouse anti-influenza primary antibody targeting NP (MAB8257, Merck) diluted with 3% BSA solution in PBS (1 μg/mL) and incubated for 1–2 h at 37°C. The detection was carried out with fluorescein isothiocyanate (FITC)-conjugated secondary rabbit anti-mouse immunoglobulin G (IgG) antibody (AP160F, Merck) diluted with 3% BSA solution in PBS (1:150) for 30–60 min at 37°C. Visualization under a fluorescence microscope was followed by calculation of fluorescent-forming units (FFU/mL).

MTT assay

MDCK cells were seeded, grown, and treated with siRNA or oligonucleotide in experiments parallel to those investigating the antiviral potential of these molecules. After a 12-h incubation in solution containing siRNAs or oligonucleotides, cultured cells were subjected to the CellTiter 96 non-radioactive cell proliferation assay (MTT) (Promega) according to the manufacturer's protocol. Measurements at a reference wavelength of 650 nm were subtracted from the recorded absorbance at 570 nm. The normalized absorbance of cells treated with selected molecules and untreated cells was compared.

Serum Stability

We performed serum stability tests on modified and unmodified siRNAs. All analyzed siRNAs were dissolved in 10% FBS solution. A ^{32}P-labeled sense strand was added to each solution. Samples were incubated for up to 2 h at 37°C, and aliquots were collected and precipitated. Then, samples were resolved (10 μL of H_2O, 10 μL of 7 M urea in 1× TBE [Tris-borate-EDTA] buffer, 0.03% bromophenol blue [BB]) and loaded on a 20% denaturing polyacrylamide gel. The gel images were obtained with a phosphorimager (Fuji FLA-5100). Bands corresponding to full-length siRNA were quantitated and compared to the sample collected and precipitated immediately after dissolving the siRNA in the FBS solution.

Stability in Lysates

Cell lysates were prepared with a PARIS kit (Invitrogen), according to the manufacturer's instructions. siRNAs were dissolved in the cell lysates, and a ^{32}P-labeled sense strand was added to each solution. Samples were incubated for up to 2 h at 37°C and treated as described for the serum stability experiment.

UV Melting Experiments

The siRNA duplexes were melted in buffer containing 100 mM NaCl, 20 mM sodium cacodylate, and 0.5 mM Na_2EDTA (pH 7). Oligonucleotide single-strand concentrations were calculated from the absorbance measured at a temperature above 80°C, and single-strand extinction coefficients were approximated by a nearest-neighbor model. Modified oligonucleotide strands with identical sequences were assumed to have identical extinction coefficients. The measurements were performed for nine different concentrations of each siRNA in the range 10^{-4}–10^{-6} M. Absorbance versus temperature melting curves were measured at 260 nm at the heating rate of 1°C/min from 0°C to 90°C using a JASCO V-650 spectrophotometer with a thermoprogrammer. The melting curves were analyzed, and the thermodynamic parameters were calculated using a two-state model with MeltWin 3.5 software.[77] For most duplexes, the ΔH° derived from TM-1 versus ln(CT/4) plots was within 15% of the value derived from averaging the fits to individual melting curves as expected if the two-state model is reasonable.

Statistical Analysis

Experimental data were analyzed with a two-tailed t test with unequal variance in Microsoft Excel software. Three intervals of statistical confidence were considered as 0.05, 0.01, and 0.001. Statistics were calculated from three independent experiments (each containing three technical repeats), normalized to virus titer from cells treated with Lipofectamine 2000 only.

SUPPLEMENTAL INFORMATION

Supplemental Information can be found online at https://doi.org/10.1016/j.omtn.2019.12.018.

AUTHOR CONTRIBUTIONS

E.K. and J.P. conceived and designed the experiments. J.P., E.L., M.S.-J., B.S., R.K. and E.K. performed the experiments. E.K., J.P. and E.L. analyzed the data. J.P. and E.K. wrote the paper.

ACKNOWLEDGMENTS

This study was supported by National Science Centre, Poland, grants UMO-2016/21/N/NZ1/00565 to J.P., UMO-2015/19/B/NZ1/02803 to E.K., UMO-2017/25/B/NZ1/02269 and UMO-2013/08/A/ST5/00295 to R.K., and UMO-2017/24/C/NZ1/00219 to E.L. This publication was also supported by the Polish Ministry of Science and Higher Education, Poland, under the KNOW program.

REFERENCES

1. Shin, W.J., and Seong, B.L. (2019). Novel antiviral drug discovery strategies to tackle drug-resistant mutants of influenza virus strains. Expert Opin. Drug Discov. *14*, 153–168.

2. Hu, Y., Sneyd, H., Dekant, R., and Wang, J. (2017). Influenza A virus nucleoprotein: a highly conserved multi-functional viral protein as a hot antiviral drug target. Curr. Top. Med. Chem. *17*, 2271–2285.

3. Samji, T. (2009). Influenza A: understanding the viral life cycle. Yale J. Biol. Med. *82*, 153–159.

4. Bouvier, N.M., and Palese, P. (2008). The biology of influenza viruses. Vaccine *26* (*Suppl 4*), D49–D53.

5. Gultyaev, A.P., Fouchier, R.A.M., and Olsthoorn, R.C.L. (2010). Influenza virus RNA structure: unique and common features. Int. Rev. Immunol. *29*, 533–556.

6. Moss, W.N., Priore, S.F., and Turner, D.H. (2011). Identification of potential conserved RNA secondary structure throughout influenza A coding regions. RNA *17*, 991–1011.

7. Priore, S.F., Kierzek, E., Kierzek, R., Baman, J.R., Moss, W.N., Dela-Moss, L.I., and Turner, D.H. (2013). Secondary structure of a conserved domain in the intron of influenza A NS1 mRNA. PLoS ONE *8*, e70615.

8. Jiang, T., Kennedy, S.D., Moss, W.N., Kierzek, E., and Turner, D.H. (2014). Secondary structure of a conserved domain in an intron of influenza A M1 mRNA. Biochemistry *53*, 5236–5248.

9. Jiang, T., Nogales, A., Baker, S.F., Martinez-Sobrido, L., and Turner, D.H. (2016). Mutations designed by ensemble defect to misfold conserved RNA structures of influenza A segments 7 and 8 affect splicing and attenuate viral replication in cell culture. PLoS ONE *11*, e0156906.

10. Moss, W.N., Dela-Moss, L.I., Kierzek, E., Kierzek, R., Priore, S.F., and Turner, D.H. (2012). The 3′ splice site of influenza A segment 7 mRNA can exist in two conformations: a pseudoknot and a hairpin. PLoS ONE *7*, e38323.

11. Gultyaev, A.P., Tsyganov-Bodounov, A., Spronken, M.I.J., van der Kooij, S., Fouchier, R.A.M., and Olsthoorn, R.C.L. (2014). RNA structural constraints in the evolution of the influenza A virus genome NP segment. RNA Biol. *11*, 942–952.

12. Ruszkowska, A., Lenartowicz, E., Moss, W.N., Kierzek, R., and Kierzek, E. (2016). Secondary structure model of the naked segment 7 influenza A virus genomic RNA. Biochem. J. *473*, 4327–4348.

13. Lenartowicz, E., Kesy, J., Ruszkowska, A., Soszynska-Jozwiak, M., Michalak, P., Moss, W.N., Turner, D.H., Kierzek, R., and Kierzek, E. (2016). Self-folding of naked segment 8 genomic rna of influenza A virus. PLoS ONE *11*, e0148281.

14. Soszynska-Jozwiak, M., Michalak, P., Moss, W.N., Kierzek, R., Kesy, J., and Kierzek, E. (2017). Influenza virus segment 5 (+)RNA—secondary structure and new targets for antiviral strategies. Sci. Rep. *7*, 15041.

15. Soszynska-Jozwiak, M., Michalak, P., Moss, W.N., Kierzek, R., and Kierzek, E. (2015). A conserved secondary structural element in the coding region of the influenza A virus nucleoprotein (NP) mRNA is important for the regulation of viral proliferation. PLoS ONE *10*, e0141132.

16. Kobayashi, Y., Dadonaite, B., van Doremalen, N., Suzuki, Y., Barclay, W.S., and Pybus, O.G. (2016). Computational and molecular analysis of conserved influenza A virus RNA secondary structures involved in infectious virion production. RNA Biol. *13*, 883–894.

17. Williams, G.D., Townsend, D., Wylie, K.M., Kim, P.J., Amarasinghe, G.K., Kutluay, S.B., and Boon, A.C.M. (2018). Nucleotide resolution mapping of influenza A virus nucleoprotein-RNA interactions reveals RNA features required for replication. Nat. Commun. *9*, 465.

18. Fournier, E., Moules, V., Essere, B., Paillart, J.C., Sirbat, J.D., Isel, C., Cavalier, A., Rolland, J.P., Thomas, D., Lina, B., and Marquet, R. (2012). A supramolecular assembly formed by influenza A virus genomic RNA segments. Nucleic Acids Res. *40*, 2197–2209.

19. Fournier, E., Moules, V., Essere, B., Paillart, J.C., Sirbat, J.D., Cavalier, A., Rolland, J.P., Thomas, D., Lina, B., Isel, C., and Marquet, R. (2012). Interaction network linking the human H3N2 influenza A virus genomic RNA segments. Vaccine *30*, 7359–7367.

20. Ferhadian, D., Contrant, M., Printz-Schweigert, A., Smyth, R.P., Paillart, J.C., and Marquet, R. (2018). Structural and functional motifs in influenza virus RNAs. Front. Microbiol. *9*, 559.

21. Simon, L.M., Morandi, E., Luganini, A., Gribaudo, G., Martinez-Sobrido, L., Turner, D.H., Oliviero, S., and Incarnato, D. (2019). In vivo analysis of influenza A mRNA secondary structures identifies critical regulatory motifs. Nucleic Acids Res. *47*, 7003–7017.

22. Michalak, P., Soszynska-Jozwiak, M., Biala, E., Moss, W.N., Kesy, J., Szutkowska, B., Lenartowicz, E., Kierzek, R., and Kierzek, E. (2019). Secondary structure of the segment 5 genomic RNA of influenza A virus and its application for designing antisense oligonucleotides. Sci. Rep. *9*, 3801.

23. Kesy, J., Patil, K.M., Kumar, S.R., Shu, Z., Yong, H.Y., Zimmermann, L., Ong, A.A.L., Toh, D.K., Krishna, M.S., Yang, L., et al. (2019). A short chemically modified dsRNA-binding PNA (dbPNA) inhibits influenza viral replication by targeting viral RNA panhandle structure. Bioconjug. Chem. *30*, 931–943.

24. Lenartowicz, E., Nogales, A., Kierzek, E., Kierzek, R., Martínez-Sobrido, L., and Turner, D.H. (2016). Antisense oligonucleotides targeting influenza A segment 8 genomic RNA inhibit viral replication. Nucleic Acid Ther. *26*, 277–285.

25. Price, A.A., Sampson, T.R., Ratner, H.K., Grakoui, A., and Weiss, D.S. (2015). Cas9-mediated targeting of viral RNA in eukaryotic cells. Proc. Natl. Acad. Sci. USA *112*, 6164–6169.

26. Asha, K., Kumar, P., Sanicas, M., Meseko, C.A., Khanna, M., and Kumar, B. (2018). Advancements in nucleic acid based therapeutics against respiratory viral infections. J. Clin. Med. *8*, E6.

27. Elbashir, S.M., Harborth, J., Weber, K., and Tuschl, T. (2002). Analysis of gene function in somatic mammalian cells using small interfering RNAs. Methods *26*, 199–213.

28. Westerhout, E.M., and Berkhout, B. (2007). A systematic analysis of the effect of target RNA structure on RNA interference. Nucleic Acids Res. *35*, 4322–4330.

29. Sagan, S.M., Nasheri, N., Luebbert, C., and Pezacki, J.P. (2010). The efficacy of siRNAs against hepatitis C virus is strongly influenced by structure and target site accessibility. Chem. Biol. *17*, 515–527.

30. Elbashir, S.M., Harborth, J., Lendeckel, W., Yalcin, A., Weber, K., and Tuschl, T. (2001). Duplexes of 21-nucleotide RNAs mediate RNA interference in cultured mammalian cells. Nature *411*, 494–498.

31. Matsuoka, Y., Matsumae, H., Katoh, M., Eisfeld, A.J., Neumann, G., Hase, T., Ghosh, S., Shoemaker, J.E., Lopes, T.J., Watanabe, T., et al. (2013). A comprehensive map of the influenza A virus replication cycle. BMC Syst. Biol. *7*, 97.

32. Te Velthuis, A.J., and Fodor, E. (2016). Influenza virus RNA polymerase: insights into the mechanisms of viral RNA synthesis. Nat. Rev. Microbiol. *14*, 479–493.

33. Lai, W.C., Kayedkhordeh, M., Cornell, E.V., Farah, E., Bellaousov, S., Rietmeijer, R., Salsi, E., Mathews, D.H., and Ermolenko, D.N. (2018). mRNAs and lncRNAs intrinsically form secondary structures with short end-to-end distances. Nat. Commun. *9*, 4328.

34. Mathews, D.H., and Turner, D.H. (2002). Dynalign: an algorithm for finding the secondary structure common to two RNA sequences. J. Mol. Biol. *317*, 191–203.

35. Fu, Y., Sharma, G., and Mathews, D.H. (2014). Dynalign II: common secondary structure prediction for RNA homologs with domain insertions. Nucleic Acids Res. *42*, 13939–13948.

36. Harmanci, A.O., Sharma, G., and Mathews, D.H. (2007). Efficient pairwise RNA structure prediction using probabilistic alignment constraints in Dynalign. BMC Bioinformatics *8*, 130.

37. Ge, Q., McManus, M.T., Nguyen, T., Shen, C.H., Sharp, P.A., Eisen, H.N., and Chen, J. (2003). RNA interference of influenza virus production by directly targeting mRNA for degradation and indirectly inhibiting all viral RNA transcription. Proc. Natl. Acad. Sci. USA *100*, 2718–2723.

38. Zhiqiang, W., Yaowu, Y., Fan, Y., Jian, Y., Yongfeng, H., Lina, Z., Jianwei, W., and Qi, J. (2010). Effective siRNAs inhibit the replication of novel influenza A (H1N1) virus. Antiviral Res. *85*, 559–561.

39. Chiu, Y.L., and Rana, T.M. (2003). siRNA function in RNAi: a chemical modification analysis. RNA *9*, 1034–1048.

40. Muhonen, P., Tennilä, T., Azhayeva, E., Parthasarathy, R.N., Janckila, A.J., Väänänen, H.K., Azhayev, A., and Laitala-Leinonen, T. (2007). RNA interference tolerates 2′-fluoro modifications at the Argonaute2 cleavage site. Chem. Biodivers. *4*, 858–873.

41. Braasch, D.A., Jensen, S., Liu, Y., Kaur, K., Arar, K., White, M.A., and Corey, D.R. (2003). RNA interference in mammalian cells by chemically-modified RNA. Biochemistry *42*, 7967–7975.

42. Choung, S., Kim, Y.J., Kim, S., Park, H.O., and Choi, Y.C. (2006). Chemical modification of siRNAs to improve serum stability without loss of efficacy. Biochem. Biophys. Res. Commun. *342*, 919–927.

43. Nowak, M., Wyszko, E., Fedoruk-Wyszomirska, A., Pospieszny, H., Barciszewska, M.Z., and Barciszewski, J. (2009). A new and efficient method for inhibition of RNA viruses by DNA interference. FEBS J. *276*, 4372–4380.

44. Lamberton, J.S., and Christian, A.T. (2003). Varying the nucleic acid composition of siRNA molecules dramatically varies the duration and degree of gene silencing. Mol. Biotechnol. *24*, 111–120.

45. Hohjoh, H. (2002). RNA interference (RNAi) induction with various types of synthetic oligonucleotide duplexes in cultured human cells. FEBS Lett. *521*, 195–199.

46. Kraynack, B.A., and Baker, B.F. (2006). Small interfering RNAs containing full 2′-*O*-methylribonucleotide-modified sense strands display Argonaute2/eIF2C2-dependent activity. RNA *12*, 163–176.

47. Amarzguioui, M., Holen, T., Babaie, E., and Prydz, H. (2003). Tolerance for mutations and chemical modifications in a siRNA. Nucleic Acids Res. *31*, 589–595.

48. Czauderna, F., Fechtner, M., Dames, S., Aygün, H., Klippel, A., Pronk, G.J., Giese, K., and Kaufmann, J. (2003). Structural variations and stabilising modifications of synthetic siRNAs in mammalian cells. Nucleic Acids Res. *31*, 2705–2716.

49. Kierzek, E., Mathews, D.H., Ciesielska, A., Turner, D.H., and Kierzek, R. (2006). Nearest neighbor parameters for Watson-Crick complementary heteroduplexes formed between 2′-*O*-methyl RNA and RNA oligonucleotides. Nucleic Acids Res. *34*, 3609–3614.

50. Schroeder, S.J. (2018). Challenges and approaches to predicting RNA with multiple functional structures. RNA *24*, 1615–1624.

51. Zhang, P., Wang, J.G., Wan, J.G., and Liu, W.Q. (2010). [Screening efficient siRNAs in vitro as the candidate genes for chicken anti-avian influenza virus H5N1 breeding]. Mol. Biol. (Mosk.) *44*, 42–50.

52. Huang, D.T., Lu, C.Y., Shao, P.L., Chang, L.Y., Wang, J.Y., Chang, Y.H., Lai, M.J., Chi, Y.H., and Huang, L.M. (2017). In vivo inhibition of influenza A virus replication by RNA interference targeting the PB2 subunit via intratracheal delivery. PLoS ONE *12*, e0174523.

53. Tompkins, S.M., Lo, C.Y., Tumpey, T.M., and Epstein, S.L. (2004). Protection against lethal influenza virus challenge by RNA interference in vivo. Proc. Natl. Acad. Sci. USA *101*, 8682–8686.

54. Ge, Q., Filip, L., Bai, A., Nguyen, T., Eisen, H.N., and Chen, J. (2004). Inhibition of influenza virus production in virus-infected mice by RNA interference. Proc. Natl. Acad. Sci. USA *101*, 8676–8681.

55. Zhou, K., He, H., Wu, Y., and Duan, M. (2008). RNA interference of avian influenza virus H5N1 by inhibiting viral mRNA with siRNA expression plasmids. J. Biotechnol. *135*, 140–144.

56. Zhou, H., Jin, M., Yu, Z., Xu, X., Peng, Y., Wu, H., Liu, J., Liu, H., Cao, S., and Chen, H. (2007). Effective small interfering RNAs targeting matrix and nucleocapsid protein gene inhibit influenza A virus replication in cells and mice. Antiviral Res. *76*, 186–193.

57. Zhang, W., Wang, C.Y., Yang, S.T., Qin, C., Hu, J.L., and Xia, X.Z. (2009). Inhibition of highly pathogenic avian influenza virus H5N1 replication by the small interfering RNA targeting polymerase A gene. Biochem. Biophys. Res. Commun. *390*, 421–426.

58. Li, W., Yang, X., Jiang, Y., Wang, B., Yang, Y., Jiang, Z., and Li, M. (2011). Inhibition of influenza A virus replication by RNA interference targeted against the PB1 subunit of the RNA polymerase gene. Arch. Virol. *156*, 1979–1987.

59. Kim, B., Park, J.H., and Sailor, M.J. (2019). Rekindling RNAi therapy: materials design requirements for in vivo siRNA delivery. Adv. Mater. *31*, e1903637.

60. Smith, C.I.E., and Zain, R. (2019). Therapeutic oligonucleotides: state of the art. Annu. Rev. Pharmacol. Toxicol. *59*, 605–630.

61. Prakash, T.P., Allerson, C.R., Dande, P., Vickers, T.A., Sioufi, N., Jarres, R., Baker, B.F., Swayze, E.E., Griffey, R.H., and Bhat, B. (2005). Positional effect of chemical modifications on short interference RNA activity in mammalian cells. J. Med. Chem. *48*, 4247–4253.

62. Kandeel, M., and Kitade, Y. (2018). Molecular dynamics and binding selectivity of nucleotides and polynucleotide substrates with EIF2C2/Ago2 PAZ domain. Int. J. Biol. Macromol. *107* (Pt B), 2566–2573.

63. Kandeel, M., Al-Taher, A., Nakashima, R., Sakaguchi, T., Kandeel, A., Nagaya, Y., Kitamura, Y., and Kitade, Y. (2014). Bioenergetics and gene silencing approaches for unraveling nucleotide recognition by the human EIF2C2/Ago2 PAZ domain. PLoS ONE *9*, e94538.

64. Geary, R.S., Norris, D., Yu, R., and Bennett, C.F. (2015). Pharmacokinetics, biodistribution and cell uptake of antisense oligonucleotides. Adv. Drug Deliv. Rev. *87*, 46–51.

65. Zheng, J., Zhang, L., Zhang, J., Wang, X., Ye, K., Xi, Z., Du, Q., and Liang, Z. (2013). Single modification at position 14 of siRNA strand abolishes its gene-silencing activity by decreasing both RISC loading and target degradation. FASEB J. *27*, 4017–4026.

66. Parrish, S., Fleenor, J., Xu, S., Mello, C., and Fire, A. (2000). Functional anatomy of a dsRNA trigger: differential requirement for the two trigger strands in RNA interference. Mol. Cell *6*, 1077–1087.

67. Smalheiser, N.R., and Gomes, O.L. (2014). Mammalian Argonaute-DNA binding? Biol. Direct *10*, 27.

68. Palauqui, J.C., and Balzergue, S. (1999). Activation of systemic acquired silencing by localised introduction of DNA. Curr. Biol. *9*, 59–66.

69. Voinnet, O., Vain, P., Angell, S., and Baulcombe, D.C. (1998). Systemic spread of sequence-specific transgene RNA degradation in plants is initiated by localized introduction of ectopic promoterless DNA. Cell *95*, 177–187.

70. Wu, S.Y., Yang, X., Gharpure, K.M., Hatakeyama, H., Egli, M., McGuire, M.H., Nagaraja, A.S., Miyake, T.M., Rupaimoole, R., Pecot, C.V., et al. (2014). 2′-OMe-phosphorodithioate-modified siRNAs show increased loading into the RISC complex and enhanced anti-tumour activity. Nat. Commun. *5*, 3459.

71. Kierzek, E., and Kierzek, R. (2003). The thermodynamic stability of RNA duplexes and hairpins containing N^6-alkyladenosines and 2-methylthio-N^6-alkyladenosines. Nucleic Acids Res. *31*, 4472–4480.

72. Xia, T., SantaLucia, J., Jr., Burkard, M.E., Kierzek, R., Schroeder, S.J., Jiao, X., Cox, C., and Turner, D.H. (1998). Thermodynamic parameters for an expanded nearest-neighbor model for formation of RNA duplexes with Watson-Crick base pairs. Biochemistry *37*, 14719–14735.

73. Kierzek, E., and Kierzek, R. (2003). The synthesis of oligoribonucleotides containing N6-alkyladenosines and 2-methylthio-N6-alkyladenosines via post-synthetic modification of precursor oligomers. Nucleic Acids Res. *31*, 4461–4471.

74. Chomczynski, P., and Sacchi, N. (2006). The single-step method of RNA isolation by acid guanidinium thiocyanate-phenol-chloroform extraction: twenty-something years on. Nat. Protoc. *1*, 581–585.

75. Dovas, C.I., Papanastassopoulou, M., Georgiadis, M.P., Chatzinasiou, E., Maliogka, V.I., and Georgiades, G.K. (2010). Detection and quantification of infectious avian influenza A (H5N1) virus in environmental water by using real-time reverse transcription-PCR. Appl. Environ. Microbiol. *76*, 2165–2174.

76. Vester, D., Lagoda, A., Hoffmann, D., Seitz, C., Heldt, S., Bettenbrock, K., Genzel, Y., and Reichl, U. (2010). Real-time RT-qPCR assay for the analysis of human influenza A virus transcription and replication dynamics. J. Virol. Methods *168*, 63–71.

77. McDowell, J.A., and Turner, D.H. (1996). Investigation of the structural basis for thermodynamic stabilities of tandem GU mismatches: solution structure of $(rGAGGUCUC)_2$ by two-dimensional NMR and simulated annealing. Biochemistry *35*, 14077–14089.

OMTN, Volume *19*

Supplemental Information

RNA Secondary Structure Motifs of the Influenza A Virus as Targets for siRNA-Mediated RNA Interference

Julita Piasecka, Elzbieta Lenartowicz, Marta Soszynska-Jozwiak, Barbara Szutkowska, Ryszard Kierzek, and Elzbieta Kierzek

Table S1. Primers and probe used in the experiments.

Primer for gene-specific reverse transcription	
	ATGAGTCTTCTAACCGAGGTCG
Primers for real-time PCR	
forward	AGACCAATCTTGTCACCTCTGAC
reverse	AGGGCATTTTGGACAAAGCGTCTACG
Probe for real-time PCR	
	FAM-TCACCGTGCCCAGTGAGCGAGGACTGC-TAMRA

All oligonucleotides are DNA. FAM – 5'end labelled with 5-FAM; TAMRA – 3'end labelled with 6-TAMRA.

Table S2. Conserved base pairs[1] used as constraints for determination of A/California/04/2009 (H1N1) (+)RNA5 folding in Dynalign mode of RNAstructure 6.1 which were incorporated to guide folding of (+)RNA5 from strain A/Vietnam/1203/2004 (H5N1).

Table S3. A/California/04/2009 (H1N1) sequence conservation among influenza type A strains in siRNA target regions**.**

siRNA name	Target region*	Sequence conservation (%)
1498	1498-1516	96.6
1342	1342-1360	76.7
1312	1312-1330	90.0
1090	1090-1108	72.9
1008	1008-1026	88.4
901	901-919	82.6
682	682-700	79.5
613	613-631	82.7
471	471-489	85.3
448	448-466	92.4
412	412-430	89.9
183	183-201	92.5

* (+)RNA5 nucleotide numbering from 5' end

Table S4. Thermodynamic parameters of duplex formation[a]

	Average of curve fits				T_M^{-1} vs log C_T plots					
siRNA	**$-\Delta H^o$ (kcal/mol)**	**$-\Delta S^o$ (eu)**	**$-\Delta G^o_{37}$ (kcal/mol)**	**T_M [b] (^{o}C)**	**$-\Delta H^o$ (kcal/mol)**	**$-\Delta S^o$ (eu)**	**$-\Delta G^o_{37}$ (kcal/mol)**	**T_M[b] (^{o}C)**	**$-\Delta\Delta G^o_{37}$ (kcal/mol)**	**ΔT_M[b] (^{o}C)**
183	143.9 ± 6.08	398.3 ± 18.1	20.38 ± 0.51	70.0	98.8 ± 4.2	265.3 ± 12.5	16.59 ± 0.36	72.1	0	0
183-sF1	86.09 ± 5.891	229.8 ± 17.3	14.80 ± 0.52	69.9	91.6 ± 4.9	246.4 ± 14.7	15.26 ± 0.39	69.6	1.33	-2.5
183-sF2	151.0 ± 18.7	411.4 ± 54.9	23.43 ± 1.72	76.1	99.03 ± 8.9	261.1 ± 25.9	18.04 ± 0.95	77.8	-1.45	5.7
471	161.6 ± 9.4	440.2 ± 27.1	25.08 ± 0.99	77.2	158.12 ± 14.2	430.1 ± 41.0	24.70 ± 1.51	77.3	0	0
471-sMe1	62.3 ± 4.7	161.5 ± 14.5	12.28 ± 0.29	68.5	64.7 ± 14.1	168.4 ± 42.2	12.48 ± 1.30	68.4	12.22	-8.9
471-sF1	80.6 ± 4.9	210.3 ± 14.0	15.46 ± 0.63	75.6	85.6 ± 14.8	224.6 ± 43.1	15.93 ± 1.49	75.2	8.77	-2.1
471-sF2	144.7 ± 9.7	385.8 ± 27.8	25.10 ± 1.18	82.6	143.6 ± 29.6	382.6 ± 83.4	24.98 ± 3.83	82.7	-0.28	5.4
613	156.8 ± 6.1	433.0 ± 17.9	22.58 ± 0.58	72.3	143.7 ± 10.3	394.3 ± 30.4	21.39 ± 0.94	72.8	0	0
613-sMe2	60.3 ± 4.9	159.51 ± 14.7	10.82 ± 0.42	60.8	63.6 ± 7.9	169.5 ± 24.1	11.02 ± 0.51	60.5	10.37	-12.3
613-sF1	163.2 ± 8.0	444.5 ± 23.0	25.34 ± 0.89	77.4	168.3 ± 25.0	459.3 ± 72.0	25.91 ± 2.73	77.3	-4.52	4.5
613-aF1	127.8 ± 14.5	337.86 ± 41.2	23.02 ± 1.76	82.9	126.9 ± 17.7	335.3 ± 50.5	22.96 ± 2.15	83.1	-1.57	10.3
613-asF1	181.5 ±1.1	483.9 ± 3.0	31.49 ± 0.22	86.4	136.8 ± 0.1	357.8 ±0.1	25.87±0.01	88.1	-4.48	15.3
613-sPS	160.9 ± 7.6	445.2 ± 22.6	22.82 ± 0.67	71.9	159.1 ± 24.5	439.9 ± 71.6	22.68 ± 2.40	72.0	-1.29	-0.8
613-aPS	167.8 ± 25.2	465.3 ± 73.5	23.47 ± 2.38	71.8	150.0 ± 15.2	413.1 ± 44.5	21.88 ± 1.40	72.4	-0.49	-0.4
613-asPS	151.8 ± 7.3	418.6 ± 21.6	21.99 ± 0.67	72.1	150.6 ± 19.5	415.1 ± 56.8	21.90 ± 1.89	72.2	-0.51	-0.6

a – solutions: 100 mM NaCl, 20 mM sodium cacodylate, 0.5 mM Na_2EDTA, pH 7, b - calculated for 10^{-4} M oligomer concentration.

REFERENCE

1. Soszynska-Jozwiak, M, Michalak, P, Moss, WN, Kierzek, R, Kesy, J, and Kierzek, E (2017). Influenza virus segment 5 (+) RNA - secondary structure and new targets for antiviral strategies. *Sci Rep* **7:** 15041.